



**Politécnico
de Viseu**

Escola Superior
de Tecnologia
e Gestão de Viseu

Trabalho efetuado sob a orientação de



**Politécnico
de Viseu**

Escola Superior
de Tecnologia
e Gestão de Viseu

Trabalho efetuado sob a orientação de

ACKNOWLEDGMENTS

To conclude, in this brief space, I would like to express my gratitude to all the people who, for whatever reason, have helped me along the way. Since it would be impossible to name and number each of the individuals who have passed through my life, I would like to offer my warmest thanks to all the individuals who have helped me grow during this period.

I leave my deep gratitude to my advisor, Professor Ricardo Almeida, for his kindness and advice. He was generous enough to provide his extensive experience and sensitivity, and believed in me from the beginning, which was a condition for the success of this work.

I express my gratitude to Professor Dr. Wellington Mazer for the learning offered on the subject, which helped me and added value to my studies and professional life. Your contribution was invaluable.

I also thank Professor Eva Barreira, who, for encouragement and additional contribution, greatly improved this work. Your help and advice were vital in improving the success of this work.

I would like to thank UTFPR and IPV for the opportunity to complete my degree with the master's program on Portuguese soil, under the double degree program, which made my university experience even more rewarding.

I offer the greatest appreciation to my parents, Jorge Augusto Serafim and Cinara Serafim, for their love and unconditional support during this long and arduous process. My father, being a permanent source of inspiration in work and success, is my hero. Thank you for your hard work and sacrifice over the years.

I would like to thank my partner, Ana Gabriela, for the unconditional support, patience and inspiration she has given me during all these years, especially in the last year. Your encouragement and understanding were very necessary for me to be able to fully concentrate on this project.

I also thank my friends and family for always being available and for offering encouragement and moral support. Our conversations and moments of relaxation were essential to maintain balance during this period.

AGRADECIMENTOS

Para concluir, neste breve espaço, gostaria de expressar meu agradecimento a todas as pessoas que, por qualquer motivo, me ajudaram ao longo do caminho. Como seria impossível nomear e numerar cada um dos indivíduos que passaram pela minha vida, gostaria de oferecer meus mais calorosos agradecimentos a todos os indivíduos que ajudaram no meu crescimento neste período.

Deixo a minha profunda gratidão ao meu orientador, Professor Ricardo Almeida, pela sua gentileza e conselhos. Ele foi generoso o suficiente para fornecer sua ampla experiência e sensibilidade, e acreditou em mim desde o início, o que foi uma condição para o sucesso deste trabalho.

Expresso a minha gratidão ao Professor Dr. Wellington Mazer pelo aprendizado oferecido sobre o assunto, que me ajudou e agregou valor aos meus estudos e vida profissional. Sua contribuição foi inestimável.

Também agradeço a professora Eva Barreira, que, por incentivo e contribuição adicional, melhorou amplamente este trabalho. Sua ajuda e conselhos foram vitais para melhorar o sucesso deste trabalho.

Gostaria de agradecer à UTFPR e ao IPV pela oportunidade de concluir a minha graduação com o programa de mestrado em solo português, no âmbito do programa de dupla diplomação, o que tornou a minha experiência universitária ainda mais gratificante.

Ofereço o maior apreço aos meus pais, Jorge Augusto Serafim e Cinara Serafim, pelo amor e apoio incondicional durante este longo e árduo processo. Meu pai, sendo uma fonte permanente de inspiração no trabalho e no sucesso, é meu herói. Agradeço o vosso trabalho árduo e seu sacrifício durante estes anos.

Gostaria de agradecer à minha companheira, Ana Gabriela, pelo apoio incondicional, paciência e inspiração que ela me deu durante todos esses anos, principalmente no último ano. Seu encorajamento e compreensão foram muito necessários para que eu pudesse me concentrar totalmente neste projeto.

Também reconheço meus amigos e familiares por estarem disponíveis em todos os momentos e por oferecerem encorajamento e apoio moral. Nossas conversas e momentos de descontração foram essenciais para manter o equilíbrio durante este período.

ABSTRACT

The application of thermography, as a non-destructive technique to evaluate pathologies in buildings where destructive tests are unfeasible or difficult to perform, stands out as a valuable tool with high potential. InfraRed Thermography (IRT) offers the ability to identify structural pathologies and abnormalities by inspecting thermal radiation from building surfaces. While widespread, the applicability of IRT is generally constrained by the quality of the resultant thermal images as well as their interpretative subjectivity. The aim of this research is to circumvent these shortcomings by developing an automatic system for the identification of construction pathologies using thermal images, which would make building inspections more accurate and efficient.

The approach employed in this work involved the collection and categorization of a database of thermal images, which served as the foundation for developing the automatic detection tool. The research process was structured into several primary phases, including problem definition, data collection, image processing, implementation of software, and assessment.

The results of this study confirmed the instrument to be useful in detecting and mapping construction irregularities. The presence of noise in the thermal images, nonetheless, posed a significant threat to the accuracy of the detection process. Comparative studies indicated that color detection methods outperformed percentile-based methods in terms of accuracy and reliability. The image processing functions were highlighted, although drawbacks like fixed resolution and potential memory utilization issues were noted.

In conclusion, this research contributes to automated pathology detection in building diagnostics using infrared thermography. The developed tool can potentially assist technicians with a more efficient and objective means of interpreting thermal images. The tool's performance should be further enhanced, with the inclusion of machine learning algorithms for improved accuracy, and the database populated to enable stronger neural network training. Additionally, the incorporation of a report features to categorize discovered pathologies by extent of damage would also make the tool more realistically functional.

Keywords: Automatic detection; InfraRed Thermography; InfraRed images.

RESUMO

A aplicação da termografia, como técnica não destrutiva para avaliar patologias em edificações onde os ensaios destrutivos são inviáveis ou de difícil execução, destaca-se como uma ferramenta valiosa e de alto potencial. A termografia infravermelha (IRT) oferece a capacidade de identificar patologias e anormalidades estruturais inspecionando a radiação térmica das superfícies dos edifícios. Embora difundida, a aplicabilidade é geralmente limitada pela qualidade das imagens térmicas resultantes, bem como por sua subjetividade interpretativa. O objetivo desta pesquisa é contornar essas deficiências desenvolvendo um sistema automático para a identificação de patologias construtivas usando imagens térmicas, o que tornaria as inspeções prediais mais precisas e eficientes.

A abordagem empregada neste trabalho envolveu a coleta e categorização de um banco de dados de imagens térmicas, que serviu de base para o desenvolvimento da ferramenta de detecção automática. O processo de pesquisa foi estruturado em várias fases primárias, incluindo definição do problema, coleta de dados, processamento de imagens, implementação de software e avaliação.

Os resultados deste estudo confirmaram que o programa é útil na detecção e mapeamento de irregularidades na construção. A presença de ruído nas imagens térmicas, no entanto, representou uma ameaça significativa à precisão da detecção. Estudos comparativos indicaram que os métodos de detecção de cores superaram os métodos baseados em percentil, em termos de precisão e confiabilidade. O processamento de imagem fora destacado, embora tenham sido observadas desvantagens como resolução fixa e possíveis problemas de utilização de memória.

Em conclusão, esta pesquisa contribui para a detecção automática de patologias em edifícios usando termografia infravermelha. A ferramenta desenvolvida pode auxiliar técnicos com um meio mais eficiente e objetivo de interpretar imagens térmicas. O desempenho da ferramenta deve ser aprimorado ainda mais, com a inclusão de aprendizado de máquina para maior precisão e banco de dados para permitir um treinamento da rede neural. Além disso, recomenda-se a incorporação de funcionalidades de relatório que permitam categorizar as patologias identificadas conforme a extensão dos danos observados.

Palavras-chave: Detecção automática; Termografia infravermelha; Imagens termográficas.

SUMMARY

1. INTRODUCTION	13
1.1. FRAMING.....	13
1.2. RESEARCH OBJECTIVES.....	13
1.2.1. <i>General Objective</i>	13
1.2.2. <i>Specific Objectives</i>	13
1.3. METHODOLOGICAL APPROACH.....	14
1.4. THESIS STRUCTURE.....	15
2. STATE OF THEART.....	16
2.1. FUNDAMENTALS	16
2.1.1. <i>Importance of the inspection for the preservation of buildings</i>	16
2.1.2. <i>Durability of concrete and the effect of water</i>	16
2.1.3. <i>InfraRed Thermography</i>	20
2.1.4. <i>Image interpretation: Passive vs Active and Qualitative VS Quantitative</i>	22
2.1.5. <i>New approaches to automatic detection/pattern recognition in IRT</i>	23
2.2. SYSTEMATIC REVIEW	24
2.2.1. <i>Inclusion and exclusion criteria</i>	26
2.2.2. <i>Main findings of the results</i>	29
3. METODOLOGY	34
3.1. PROBLEM DEFINITION	34
3.2. THE DATABASE	34
3.3. SOFTWARE DEVELOPMENT	34
3.4. CALIBRATION AND PRE-PROCESSING.....	35
3.5. ANOMALIE DETECTION	36
3.6. DATA EXPORT	37
3.7. JUSTIFICATION OF THE APPROACH.....	37
3.8. PROGRAM IMPLEMENTATION.....	38
3.8.1. <i>Key features</i>	38
3.8.1.1. Image Upload.....	38
3.8.1.2. Image processing.....	39
3.8.1.3. Temperature Calibration	41
3.8.1.4. Colormap.....	43
3.8.1.5. Definition of the Analysis Area	53
3.8.1.6. Temperature Segmentation	54
3.8.1.7. Anomalies detection.....	56

3.8.1.8.	Clear Image.....	60
3.8.1.9.	Segment Info.....	60
3.8.1.10.	Export Temperature Matrix.....	61
3.8.1.11.	Open.....	61
3.8.1.12.	Save.....	62
4.	ANALYSIS OF THE RESULTS.....	63
4.1.	PRE-PROCESSING AND NOISE REMOVAL	63
4.2.	TEMPERATURE CALIBRATION	65
4.3.	CHANGE COLORMAP	67
4.4.	USING IMAGE COLORS	68
4.5.	DEFINE ANALYSIS AREA.....	69
4.6.	SET CUSTOMS INTERVALS.....	70
4.7.	DETECT ANOMALIES	71
4.8.	DETECT COLORS.....	72
4.9.	SHOW SEGMENT INFO.....	73
4.10.	CLEAR IMAGE.....	76
4.11.	EXPORT MATRIX.....	76
5.	CONCLUSION AND FUTURE WORKS.....	77
	REFERENCES	79
6.	ANNEX.....	86
6.1.	ANNEX A – IMAGENS DE REFERÊNCIA UTILIZADAS NO PROGRAMA	87
6.2.	ANNEX B – RESULTS OF USING DETECT ANOMALIES	90
6.3.	ANNEX C- RESULT OF USING DETECT COLORS	94

LIST OF TABLES

Table 1- Keywords selection for machine learning systematic literature review.	26
Table 2 - Authors and Articles.	29
Table 3- Result of segment information.	75
Table 4- Information of color detect areas.	75
Table 5- Statistical data of the analysed area.	76

LIST OF FIGURES

Figure 1- Methodology flowchart.....	14
Figure 2- Cracking of concrete [18].	18
Figure 3- Diagram of the formation of efflorescence on concrete. Adapted from [20].	18
Figure 4- Types of corrosion of a steel bar [18].	19
Figure 5- Development of the alkali-aggregate reaction in concrete. Adapted from [18].	20
Figure 6- Thermal imaging.....	21
Figure 7- The systematic review processes [51].	25
Figure 8- Distribution According to Countries of Origin.....	27
Figure 9- Keywords co-occurrence analysis map of the reviewed articles [52].	28
Figure 10- Keywords of the chosen articles [52].	28
Figure 11- Flow chart of the program.	34
Figure 12- Window of the startup of the program.....	39
Figure 13- Remove Noise function	40
Figure 14- Apply Color Map function.....	41
Figure 15- Home of the program before calibration.....	42
Figure 16- Menu of the calibrate temperature.	42
Figure 17- Home of the program after calibration.	43
Figure 18- Temperature of the pixel.....	43
Figure 19- Colors of plasma.	44
Figure 20- Colors of inferno.....	45
Figure 21- Colors of magma.....	46
Figure 22- Colors of cividis.....	47
Figure 23- Colors of coolwarm.	47
Figure 24- Colors of spring.	48

Figure 25- Colors of autumn.	49
Figure 26-Colors of jet.	50
Figure 27- Colors of Viridis.	51
Figure 28- Definition of the area of analysis.	54
Figure 29- Auto Segment function.	55
Figure 30- Menu of the Set Custom Range.	56
Figure 31- Image after the definition of the interval and number of steps.	56
Figure 32- Definition of the percentile for anomalies detection	57
Figure 33- Detect possible anomalies using percentile function.	58
Figure 34- Detect possible anomalies in a defined area.	58
Figure 35- Detection using colors patterns.	59
Figure 36- Detection using colors patterns only in a specific area of the image.	59
Figure 37- Clear image menu.	60
Figure 38- Segment Information.	61
Figure 39- Reference image.	64
Figure 40- Image before remove noise.	64
Figure 41- Image after remove noise.	64
Figure 42- Calibrate temperature.	66
Figure 43- Black and white image.	68
Figure 44- Coloured image.	68
Figure 45- Image after using image colors.	69
Figure 46- Image that contains many anomalies.	70
Figure 47- Only the selected portion of the window.	70
Figure 48- Image after the set custom intervals.	71
Figure 49- Defined interval.	71

Figure 50- Visual comparison illustrating anomaly detection: (a) original thermal image and (b) image processed with the detect anomalies function.	72
Figure 51- Visual comparison illustrating anomaly detection: (a) original thermal image and (b) image processed with the detect colors function.....	73
Figure 52- Reference image for the show segment info.....	75
Figure 53- Image of the area selected for analysis.	75
Figure 54- Range of temperatures to choose.	75

ACRONYMS

ACI American Concrete Institute

AEs autoencoders

BMP BitMaP

CNNs Convolutional Neural Networks

CSV Comma-Separated Value

EXIF Exchangeable Image File Format

fMs Temperature Factors Maximum

fms Temperature Factors Minimum

fRs Temperature Factors

GANs Generative Adversarial Networks

GIF

IR InfraRed

IRT InfraRed Thermography

IS2 Intelligence Specialist Petty Officer 2nd Class

ITF Improved Temperature Factor

JPG Joint Photographic Experts Group

MEEMD Multidimensional Empirical Mode Decomposition

NDT Non-Destructive Testing

PCA Principal Component Analysis

PKL Pickle Format

PNG Portable Network Graphics

PT Passive Thermography

RAW Unprocessed Data

RBMs Constrained Boltzmann Machines

REBAP Regulation of Reinforced and Prestressed Concrete Structures

RGB Red, Green, Blue

RNNs Recurrent Neural Networks

TA Active Thermography

TI Temperature Index

TIFF Tag Image File Format

UAS Unmanned Aerial Systems

1. INTRODUCTION

1.1. Framing

The use of inspection and diagnostic techniques that are non-destructive and capable of assessing pathologies in buildings is of great value, since a lack of prevention and consequent late and/or wrong maintenance can significantly impact on the performance of buildings with possible relevant economic consequences [1].

Infrared thermography (IRT) has stood out when it comes to detecting pathologies without the use of destructive means [2]. However, its effectiveness can be affected as it requires a rigorous interpretation and analysis of the data collected and made by specialized technicians [3].

In addition, the quality of the images themselves can be an additional factor of uncertainty that conditions the evaluation. In this sense, the automation of this interpretation presents itself as a solution to minimize evaluation errors. In thermal image processing, the application of techniques aimed at detecting specific anomalies presents additional challenges [4].

For example, images captured by RGB cameras or visible spectrum-sensitive cameras have a higher resolution than cameras used in IRT applications, conditioning the direct use of available tools for the processing of real images [5].

In this work the intent is to develop a tool that allows the identification, mapping and classification of pathologies in buildings, based on criteria of the limit conditions of surface temperature variation. This task will be supported in a compilation and organization of a set of thermal images, which will work as database.

1.2. Research objectives

1.2.1. General Objective

The main objective of this research is to develop a software tool for the analysis and processing of thermal images, aimed at the automatic detection and identification of building pathologies.

1.2.2. Specific Objectives

To achieve the main objective, a set of specific objectives were established:

- Compile and organize a set of thermal images that work as a database to support the development of the tool.
- Establish limit conditions for temperature variation that allow the identification and mapping of pathologies.
- Program the conditions established in a tool and test it in at least two case studies.

1.3. Methodological approach

The progression of this research assumed a methodical flow that starts with thermal image acquisition and processing, leading to field deployment and validation of software created for automated pathology detection. The process implemented can be outlined in the phases below and in the Figure 1:

- Problem Identification and Objectives:
 - The determination of constraints encountered in the evaluation of pathologies in buildings.
 - Formulation of guidelines for the automation of the detection process.
- Data collection:
 - Utilization of thermal imagery of the article.
- Image processing:
 - Application of image filtering and segmentation techniques.
 - Thermal calibration for delivering precision in anomaly detection.
- Software Development:
 - Programming of pathology detection algorithm.
 - The development of a graphical interface for enhancing the usability of the tool.
- Assessment and verification:
 - Evaluation of the tool in different settings and comparison with manual testing.
 - Performance measures, i.e., hit rate.



Figure 1- Methodology flowchart.

1.4. Thesis Structure

The current research is presented in five individual chapters. Chapter 1 presents the overall topic and provides background information on the application of thermal imaging and the development of software that will contribute to the analysis of thermal images.

Chapter 2 is a literature review of thermographs and their application in building inspection and discussion regarding methods to automate anomaly detections.

Chapter 3 outlines the general research approach taken, providing information on data collection procedures, image processing tasks, and software development.

Chapter 4 presents the key findings derived and offers analysis of the data collected from the thermal images.

Chapter 5 is a reflection on the findings, their limitations, implications, and contribution to literature, and recommendations for improvement and avenues for future research.

2. STATE OF THEART

2.1. Fundamentals

2.1.1. Importance of the inspection for the preservation of buildings

Inspection is a key component in the operation and maintenance of buildings, especially in a context where the longevity and safety of the constructions are fundamental. With the increased exposure of existing structural designs to aggressive environmental agents, regular inspection has become an essential procedure to ensure the durability and integrity of buildings [6].

An inspection authorizes the initial detection of pathologies, such as cracks, corrosion of reinforcement, carbonation and other degradation situations, which can influence the structural capacity and safety of users. The inspection then contributes to preventive maintenance, avoiding short-term repair expenses and preventing fatal failures [6].

With current standards such as Eurocode 2 of 2023 and the guidelines of the American Concrete Institute (ACI) in the year 2022, the role of inspection is reinforced, highlighting the importance of continuous monitoring, recurring evaluation of buildings and certifying the safety of structures. Inspections not only ensure the safety and functionality of buildings, but also contribute to its sustainability, contributing to global waste reduction and resource conservation goals [7], [8], [9].

2.1.2. Durability of concrete and the effect of water

The consideration of the durability of concrete was not initially contemplated in the first national regulations, being introduced only with the advent of the Regulation of Reinforced and Prestressed Concrete Structures (REBAP) in 1983. Subsequently, the importance of durability was duly recognized and incorporated into the new regulations of several countries, including those of the European Union, becoming a fundamental criterion in the design of reinforced concrete structures [10]. The [11] standard establishes that a durable structure must satisfy, throughout its useful life, the requirements of use, strength, and stability, considering the actions on the structure, deformations, and environmental conditions.

Understanding and applying concrete protection techniques is of paramount importance to ensure the durability and strength of structures built with this material. Concrete, widely used in construction, is susceptible to various degradation factors over time. By

adopting preventive measures, such as regular maintenance and choosing the most appropriate techniques for specific inspection, it can contribute to the sustainability of concrete, extending its useful life and ensuring its long-term integrity [12].

The growth of civil construction has driven technological development, expanding knowledge about structures and materials through studies and analysis of previous errors. Despite this advancement, some inevitable unintentional failures persist. Structural degradation, which involves changing the shape of the structural element, results from a series of failures and factors that compromise structural performance, leading to early deterioration. Promptly identifying these pathologies is essential to prevent serious structural problems [12] [13].

With the continuous exposure of concrete structures to deteriorating agents such as water, wind, and carbon dioxide, accompanied by poor maintenance, damage is plausible. The primary causes of water infiltration in building envelopes include the penetration of rainwater, condensation, and capillary rise of groundwater in cases where the foundations are not properly waterproofed [14], [15].

These adversities can manifest themselves in a variety of ways, including biological, physical, chemical, or mechanical damage. In addition, mistakes made in the design, production, and construction phases contribute to the emergence of pathologies in structures [12]. Water is one of the causes the most significant pathologies, since it can infiltrate the concrete through pores, cracks, and capillary action, with that it can weaken the durability, structural integrity and appearance of the material. The pathologies related to water are:

Fissures and Cracks: In cold climates concrete suffers with freeze-thaw, when the water infiltrates the concrete with the expanding and formation of cracks and fissures (Figure 2). In arid climates the evaporation of the water can shrink the cracks. The cracks can make the structure weaker and create pathways for more water and aggressive agents to penetrate the concrete, causing the acceleration of the deterioration [16], [17].

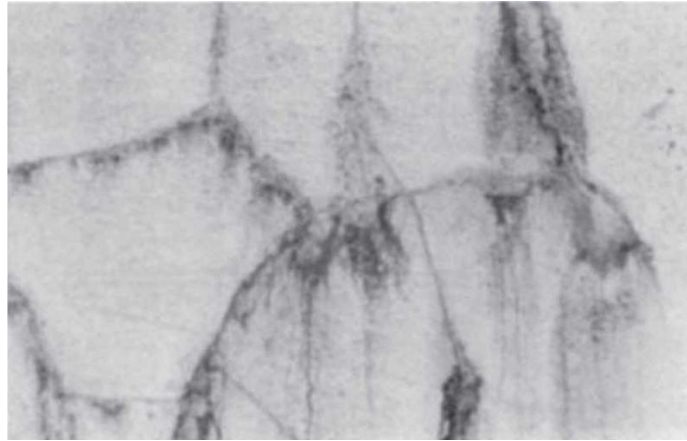


Figure 2- Cracking of concrete [18].

Efflorescence: These pathologies are made when the water dissolves the salt inside the concrete and bring them to the surface (Figure 3), these salts crystallize as the evaporation of the water occurs. Initiating white deposits compromised the aesthetic appearance of the structure. In extreme cases this efflorescence can lead to spalling or flaking, and with that can expose concrete to more damage [19].

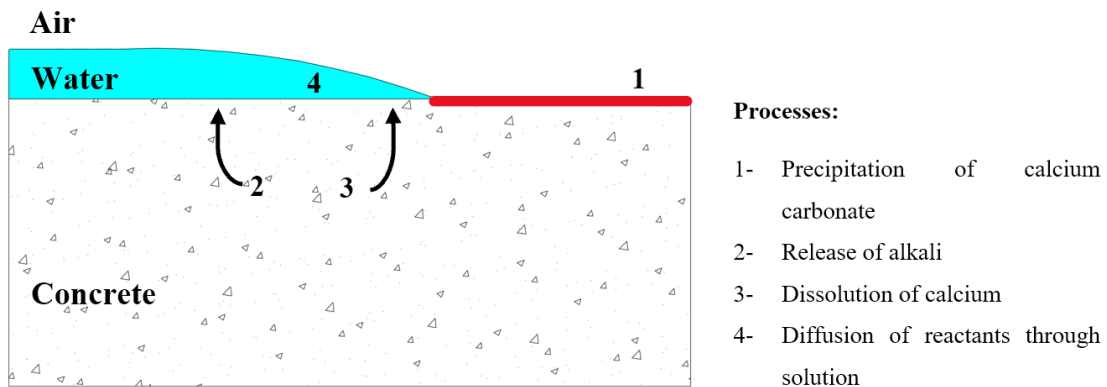


Figure 3- Diagram of the formation of efflorescence on concrete. Adapted from [20].

Corrosion of Reinforcement: This is one of the most serious pathologies that water can cause. When water penetrates the structure, especially when associated with chlorides and other types of salts, and reaches the reinforcement, the corrosion process begins, weakening the steel and expanding it, causing it to generate internal stresses, which leads to cracking in the structure, chipping, and delamination of the concrete [21], [22].

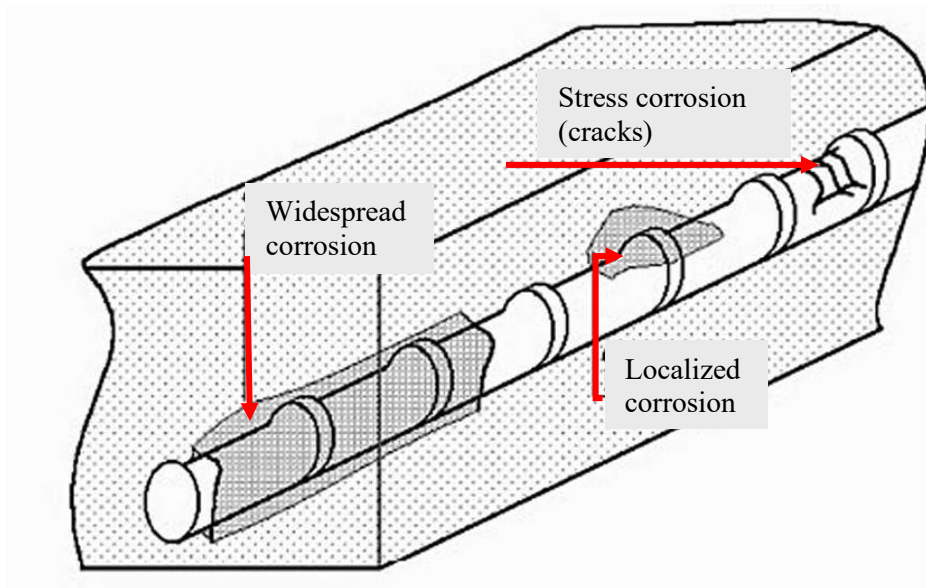


Figure 4- Types of corrosion of a steel bar [18].

Leaching: The cause of leaching occurs when water dissolves and removes calcium compounds from cement, which leads to weakening of the concrete. This type of pathology is common in structures that are exposed to running water, such as in dams, pipes, and sewage systems. This pathology over time reduces the strength of concrete and increases its permeability, making it more susceptible to other pathologies [23].

Carbonation: With water facilitating the creation of calcium carbonate due to the reaction of carbon dioxide (CO_2) found in the atmosphere, and calcium hydroxide from concrete. This combination reduces the pH of the concrete, causing the passive layer that protects the reinforcement to be destroyed, thus making the reinforcement more prone to corrosion. This process is slow, but it considerably reduces the useful life of the structure [24].

Alkali-Aggregate Reaction (AAR): In the alkali-aggregate reaction, water is the main element of the chemical process that occurs between cement alkalis and some types of aggregates. This process forms a gel that absorbs water and expands. This expansion causes internal stresses, which lead to cracks and deformations in the concrete. This pathology becomes a problem when the structure is exposed to humidity for long periods [25]. The aforementioned process is illustrated in Figure 5.

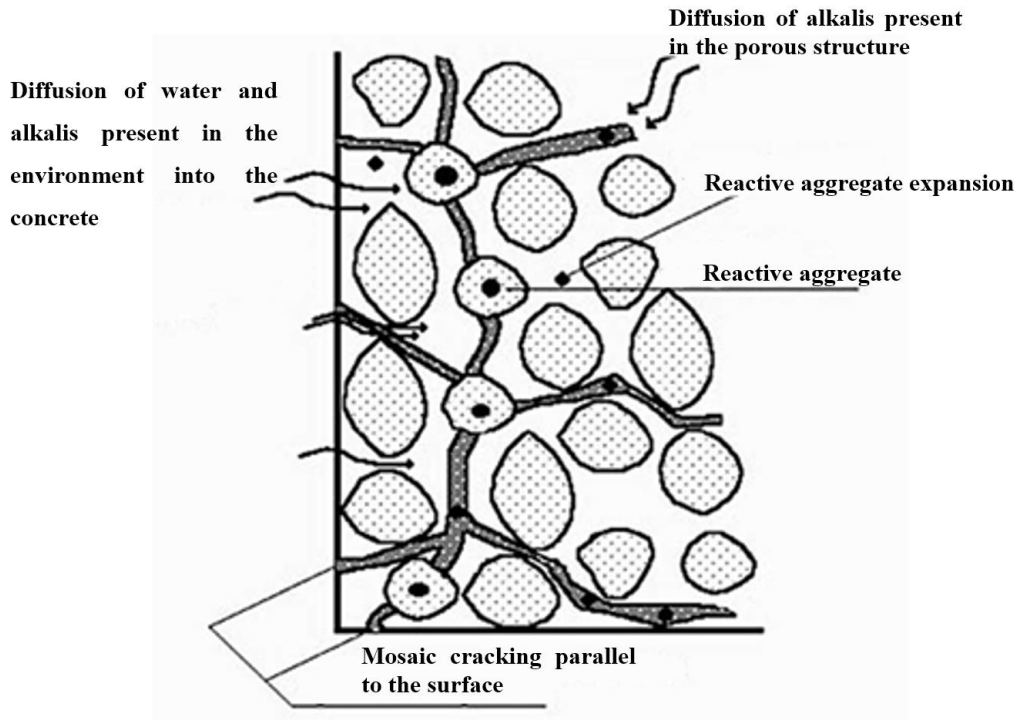


Figure 5- Development of the alkali-aggregate reaction in concrete. Adapted from [18].

Biological Growth: With the growth of microorganisms, such as algae, fungi and bacteria, caused by water on the surface of the concrete, there is a production of acids that degrade the concrete, which leads to erosion on its surface and increased porosity, which can cause other pathologies and the blockage of drainage systems, causing accumulation of water and more damage [26].

Considering the pathologies, it is essential to inspect and assess the condition of the structure. Although destructive testing methods can be employed for this purpose, their application becomes impractical if the structure is in operation. Consequently, the adoption of non-destructive techniques, such as IRT, has become necessary. This method offers significant advantages including real-time diagnosis, remote application, and the ability to assess structural conditions without causing damage [27], [28], [29], [30].

2.1.3. InfraRed Thermography

The Non-Destructive Testing (NDT) provides valuable information about buildings, supporting research applicable to various fields. This technique enables the identification of wall components, structural supports, and physical damage, facilitating a comprehensive assessment of the building's condition [3].

The IRT is based on measuring the InfraRed (IR) radiation emitted by a material by means of photoelectric sensors sensitive to the IR spectrum and installed inside an IR camera, converting it into a thermal image (single measurement) or a thermal image sequence (measurement over a specific period) [31].

IRT is a NDT that utilizes cameras to detect and measure thermal radiation emitted by objects, allowing for a direct reading of the surface temperature of the inspected subject [32]. The application of the method is conducted without physical contact, making it a non-invasive technique for obtaining important information. The results are presented as a thermogram - an electronic image that illustrates the temperature distribution across the analyzed surface (Figure 6). Besides the immediate information concerning surface temperature distribution, this type of measurement can be particularly effective in detecting air leakage, heat losses, and moisture-related issues [32], [33].

The primary advantages of this method include the ability to identify affected areas and structural defects through qualitative analysis, as well as estimate the depth of damage via quantitative assessment. Additionally, it enables remote measurements, real-time operation, and the generation of easily interpretable 2D and 3D imaging results. This technique also offers high precision, rapid scanning capabilities, and eliminates the emission of hazardous radiation, enhancing both efficiency and safety [31], [34], [35].

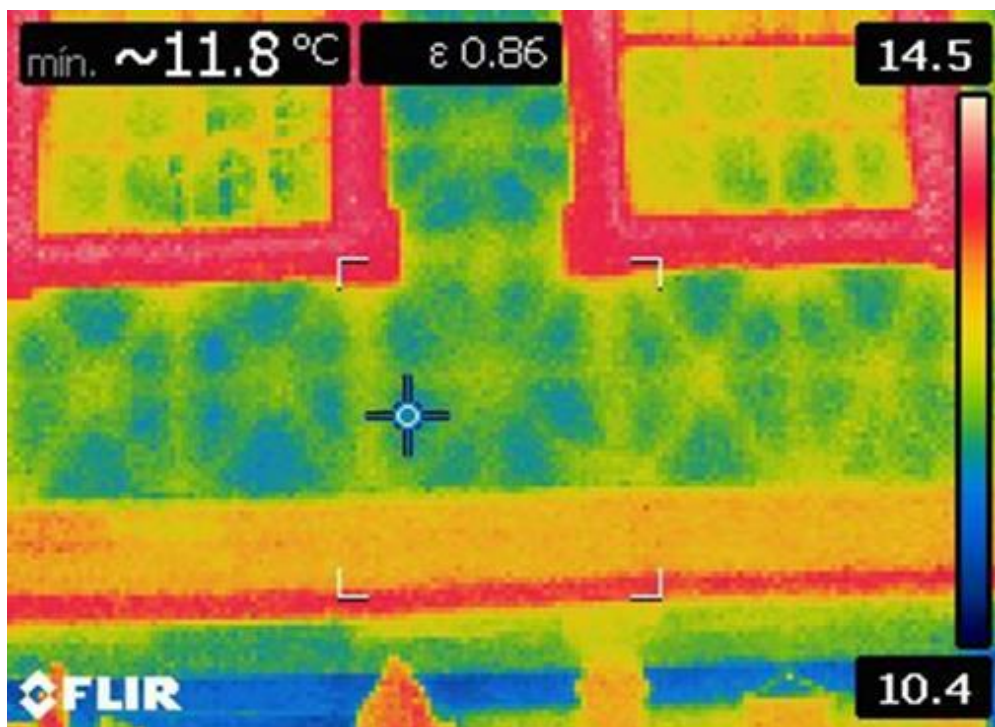


Figure 6- Thermal imaging

2.1.4. Image interpretation: Passive vs Active and Qualitative VS Quantitative

There are two possible methods of using infrared thermal imaging in buildings: passive and active. Passive IRT involves observing buildings under natural conditions, when the temperature gradient between indoor and outdoor temperatures is high enough to reveal thermal irregularities. With active InfraRed Thermography, on the other hand, the building is subjected to an external thermal stimulus, and its response is analyzed. This is a common practice in NDT of materials [36].

As for qualitative analysis versus quantitative analysis, qualitative analysis in IRT involves visual inspection of thermal images to detect anomalies such as moisture penetration, insulation gaps, and structural defects. The method leverages the observer's expertise in identifying patterns and deviations, without the need for precise measurements. As pointed out by [37], qualitative IRT is best suited for preliminary surveys and rapid inspections of large areas, making it a very practical tool for preliminary surveys of historic buildings. Furthermore, [38] demonstrated the feasibility of qualitative IRT for automated detection of moisture in various building materials and its usefulness in rapid inspections. Their flexibility and speed are suitable for qualitative analysis where immediate feedback is required, although this depends on the practitioner's experience and may not have the precision required for detailed assessments.

On the other hand, quantitative IRT analysis focuses on the measurement and quantitative assessment of thermal information, providing precise temperature values and enabling the calculation of thermal properties such as thermal resistance and heat loss. This is a prerequisite for detailed analysis such as energy audits and material testing, where accurate information is essential for effective decision making. [39] reported on the technical issues of quantitative IRT and its application in nondestructive testing and temperature measurement. [40] also used quantitative IRT to measure the thermal transmittance of non-uniform walls and demonstrated that it can provide objective and reproducible results. Although quantitative analysis has several advantages, it requires more advanced equipment and expertise and is more time-consuming than qualitative methods.

2.1.5. New approaches to automatic detection/pattern recognition in IRT

Image analysis from images acquired with IRT has conventionally been performed by visual observation and identification of pathological situations by subjective judgment. Even though the technique permits detection of moisture-affected areas, it does not provide accurate information on the geometry or severity of the damage. The practice thus introduces variability depending on the operator and compromises the overall efficiency of the inspection procedure [30]. Since inspections can deal with a huge number of images that need close and accurate examination, the constraints of manual processing become increasingly obvious.

To overcome these difficulties, various machine learning techniques have been devised to enhance data extraction from IRT images [41]. The performance of these methods has been shown to outperform others on a wide range of applications [35]. Convolutional Neural Networks (CNNs), Recurrent Neural Networks (RNNs), Autoencoders (AEs), Constrained Boltzmann Machines (RBMs), and Generative Adversarial Networks (GANs), have gradually gained application [42].

The use of such sophisticated machine learning methods makes possible the automatic detection and identification of patterns in IRT images, thus improving accuracy and efficiency of the inspection. This method not only reduces subjectivity in manual interpretation but also enhances the efficiency of handling large datasets. The [43] showed the application of neural networks for the detection of linear thermal bridges from InfraRed thermal images with high precision, recall, and F-score. This finding suggests the capability of these kinds of approaches in improving the accuracy of inspections.

Additionally, the combination of IRT with Unmanned Aerial Systems (UAS) has further extended the range of thermal inspection capabilities, especially for inaccessible areas. [44] also pointed out the application of UAS to capture thermal images of building envelopes and, by merging them with photogrammetry, the ability to generate 3D thermal models. This methodology offers an integral perspective on building thermal performance, enabling the detection of thermal irregularities and enhanced energy efficiency evaluations.

Additionally, the combination of IRT and visual inspection methods has been shown to enhance the efficiency of defect detection in buildings. [45] reported the use of IRT to detect defects such as moisture and cracking in building components, demonstrating that

although IRT is good for significant defects, it underestimates architectural defects. This calls for the application of more than one inspection method to derive a general assessment of building conditions.

Finally, the machine learning advancements and the combination of IRT with other technologies, like UAS and photogrammetry, are revolutionizing building inspection. These advancements not only increase inspection accuracy and speed but also provide useful insights into the thermal performance of buildings, helping to improve maintenance practices.

In addition, the application of multiscale analysis methods, namely empirical multidimensional set decomposition (MEEMD) when combined with principal component analysis (PCA), has proven to be effective in improving the detection of structural features in infrared thermal images [46], [47].

The technique allows for improved analysis of the thermographic data through its decomposition into various spatial scales, thereby enhancing the detection of the structural characteristics of the materials [48].

Application of object detection models enabled by deep learning, particularly those supported by TensorFlow 2.0, has been successful in thermal image analysis. Models like "EfficientDet D0 512x512" and "SSD ResNet50 V1 FPN 640x640" have performed well in classification loss and detection accuracy and can be applied in temperature tracking and security systems [49].

All these developments exemplify the potential for integrating machine learning with IRT to overcome the limitations of traditional manual inspection methods, toward more accurate and efficient solutions in building inspection and maintenance.

2.2. SYSTEMATIC REVIEW

Given the increasing interest in fields such as research, training, and education, a comprehensive literature review was conducted following the Preferred Reporting Items, for Systematic Reviews and Meta Analyses (PRISMA) protocols. This approach enhances the transparency of the research methodology and ensures the reproducibility of findings by other researchers [50].

Systematic reviews adhere to a structured set of procedures, which can be divided into distinct yet interrelated stages, as illustrated in Figure 7. Prior to conducting a review, it

is crucial to define the research question and the methodologies that will be employed to address it. This process is typically documented in a "protocol" before initiating the review. Developing a protocol or methodological plan is a fundamental step in the review process, as it enables the research team to establish a consensus on the scope of the study and the approaches to be utilized in addressing key inquiries. The level of detail and development of review protocols may vary depending on the specific requirements of the study [51].

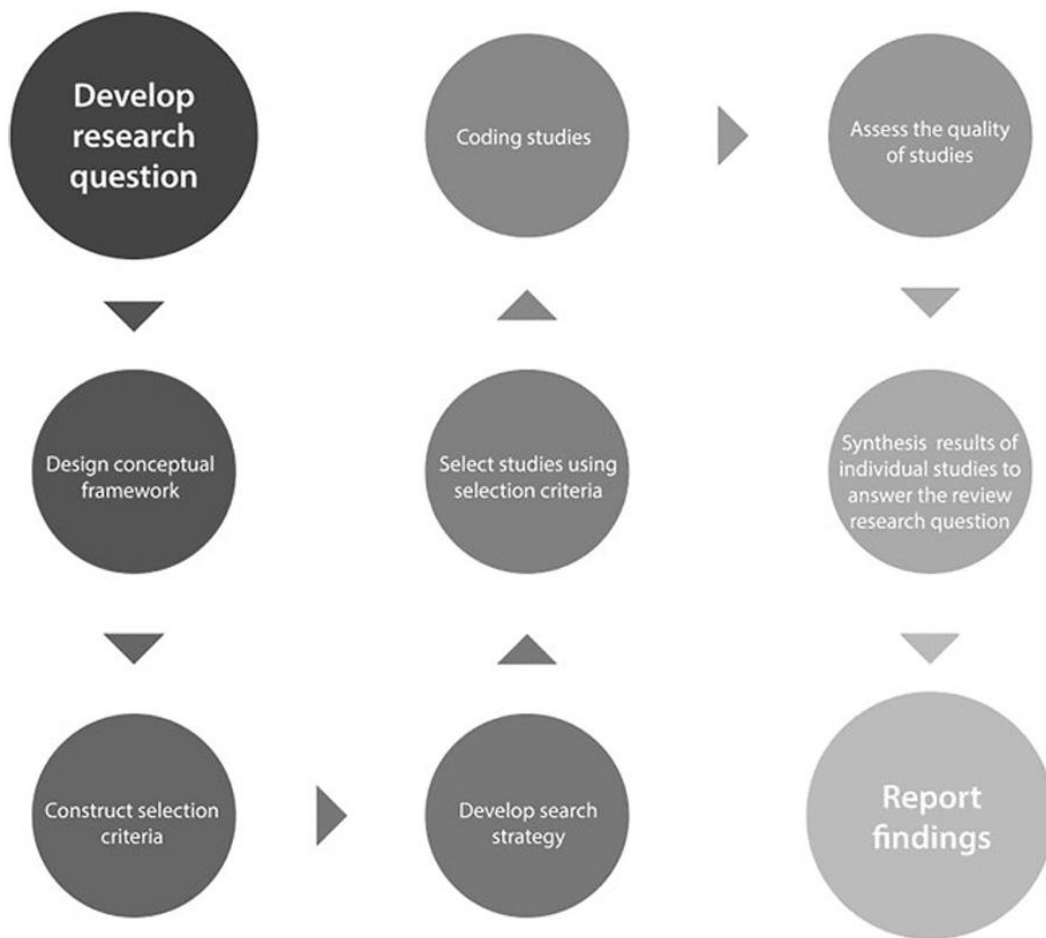


Figure 7- The systematic review processes [51].

The process began with the identification of relevant content within the Web of Science Core Collection, focusing on key phrases in the titles, abstracts, and keyword fields of the articles. A comprehensive search strategy was developed to maximize the retrieval of pertinent results. The extensive range of terms associated with decision fatigue prompted examining titles and keywords from existing review articles. This facilitated the ability to identify various spellings, word variations, synonyms, and related concepts pertaining to IRT and buildings in the context of construction. Boolean operators were employed to

refine our search, using terms such as "MUST INCLUDE" and "SHOULD INCLUDE" to ensure comprehensive coverage of all relevant focus areas, as well as wildcards ("*") to expand the scope by substituting characters and capturing multiple variations of a phrase. The three groups of keywords used in our search strategy are outlined in Table 1.

Focus	Keywords
Topic: Machine learning	"Machine learn*"
Research question: InfraRed Thermography	Building; engineering; moisture.
Purpose: Evaluation; Quantitative; Defect	Infrared thermography; quantitative infrared thermography; nondestructive evaluation; defect detection.

Table 1- Keywords selection for machine learning systematic literature review.

2.2.1. Inclusion and exclusion criteria

As previously noted, the first phase of the methodology involved conducting a keyword search across the selected databases, which resulted in the accumulation of 133 records. Subsequently, several inclusion criteria were established to filter and screen the results, as follows: i) publications dated between 2019 and January 2024 (the last five years); ii) research topics must fall within the fields of engineering, materials science, or mathematics; iii) duplicates were excluded; and iv) only journal articles were considered. Applying these criteria led to the rejection of more than half of the initially identified articles. The original set of 147 articles was thus reduced to 12 relevant sources for the research. Most of the articles found are from United States of America, with a total of 3, followed by Portugal, Spain, and South Korea, each contributing 2 articles. China, Poland, and Canada accounted with 1 article each, as shown in Figure 8.

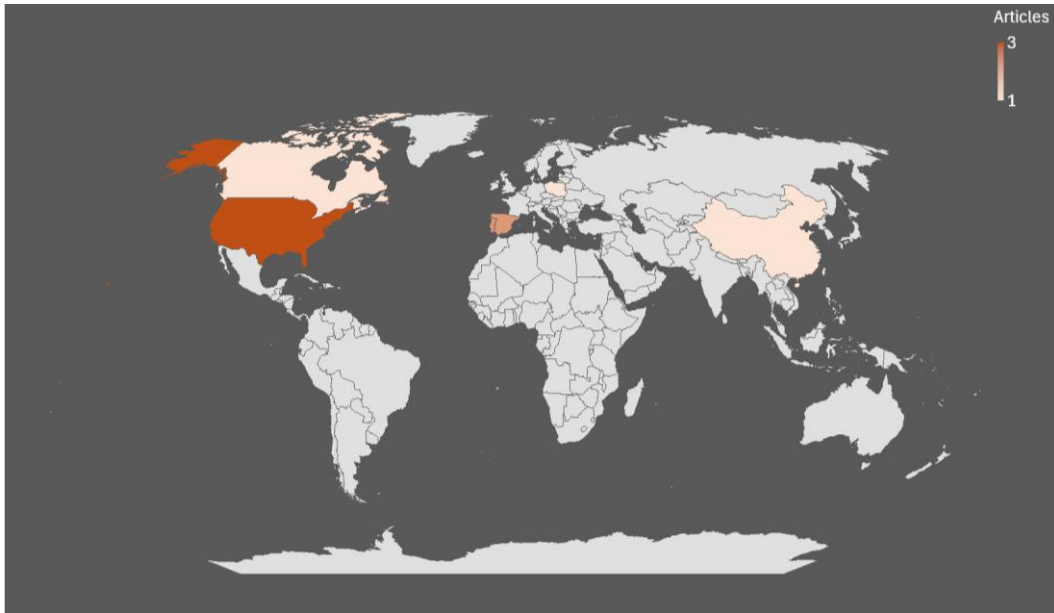


Figure 8- Distribution According to Countries of Origin.

To help explore the research themes within IRT, a visual map was generated using VOSviewer software, as shown in Figure 9. This map illustrates the relationships between terms, with node size and label reflecting the frequency of keywords, while the thickness of the lines indicates the strength of the connections between the terms. Analyzing the map of Figure 3 it is possible to observe that the main continent that writes about thermography is Europe, and the main country is Spain with 10 articles.

Prior to the application of the inclusion criteria, Figure 10 displays the bibliometric word network, representing the data before the exclusion of irrelevant articles, and the Figure 10 shows the data after the exclusion. Additionally, in the diagram, clusters or groups of items with similar or distinct characteristics are distinguished by color [50].

2.2.2. Main findings of the results

The eligible articles are presented in Table 2. It is evident that most of the articles focus on thermal imaging, with few addressing the field of automatic detection. Based on the existing literature, it can be concluded that the integration of automation in thermal imaging remains an underexplored and emerging area of research.

Authors	Title
[30] Garrido, I; Barreira, E; Almeida, RMSF; Lagueta, S	Introduction of active thermography and automatic defect segmentation in the thermographic inspection of specimens of ceramic tiling for building facades.
[43] Kim, CM; Choi, JS; Jang, H; Kim, EJ	Automatic Detection of Linear Thermal Bridges from Infrared Thermal Images Using Neural Network.
[44] Gil-Docampo, M; Sanz, JO; Guerrero, IC; Cabanas, MF	UAS IR-Thermograms Processing and Photogrammetry of Thermal Images for the Inspection of Building Envelopes.
[45] Anuar, MZT; Sarbini, NN; Ibrahim, IS; Othman, SH; Reba, MN	Building condition ratings using infrared thermography: a preliminary study.
[48] Tu, K; Ibarra-Castanedo, C; Sfarra, S; Yao, Y; Maldague, XPV	Multiscale Analysis of Solar Loading Thermographic Signals for Wall Structure Inspection.
[49] Sharrab, YO; Al-shboul, S; Alsmira, M; Khalifeh, A; Dwekat, Z; Alsmadi, I; Al-Khasawneh, A	Performance Comparison of Several Deep Learning-Based Object Detection Algorithms Utilizing Thermal Images.
[53] Almeida, ASFCE; Ornelas, AJA; Cordeiro, AMR	Passive thermography in the diagnosis of pathologies and thermal performance on building facades through a thermal camera installed on a drone. Preliminary approach in Coimbra (Portugal).
[54] Chidurala, V; Li, XR	Occupancy Estimation Using Thermal Imaging Sensors and Machine Learning Algorithms.
[55] Dafico, LCM; Barreira, E; Almeida, RMSF; Vicente, R	Machine learning models applied to moisture assessment in building materials.
[56] Li, ZS; Jin, YK; Liang, XG; Zeng, JY	Thermography evaluation of defect characteristics of building envelopes in urban villages in Guangzhou, China.
[57] Mahmoodzadeh, M; Gretka, V; Wong, S; Froese, T; Mukhopadhyaya, P	Evaluating Patterns of Building Envelope Air Leakage with Infrared Thermography.
[58] Sadhukhan, D; Peri, S; Sugunaraj, N; Biswas, A; Selvaraj, DF; Koiner, K; Rosener, A; Dunlevy, M; Goveas, N; Flynn, D; Ranganathan, P	Estimating surface temperature from thermal imagery of buildings for accurate thermal transmittance (U-value): A machine learning perspective.

Table 2 - Authors and Articles.

The methodology proposed in this study [30] focused on an alternative mode of improving accuracy while also reducing subjectivity by automating defect segmentation.

The approach was therefore divided into three stages: pre-processing, core processing, and post-processing. Images of thermal nature were segmented into smaller areas for sharpening during pre-processing. Identification of different thermal patterns based on their histogram analysis from overlapping images was done within core processing. Finally, the spatial and temporal filters used were thought to minimize false positives in post-processing. However, although the method has successfully enabled automated defect identification, this method becomes too complicated as it relies heavily on the implementation of neural networks and deep learning techniques.

The 'Automatic Detection of Linear Thermal Bridges from Infrared Thermal Images Using Neural Networks' [43] describes a procedure for the determination of linear thermal bridges in building skins through advanced image processing and machine learning approaches. The method includes clustering of thermal anomaly regions, extraction of relevant features, and application of ANN for the final thermal bridge detection. To evaluate the proposed methodology, the authors compared it against ground truth data to reach high precision, recall, and F-score values. It indicates that the technique which comprises image processing and machine learning approaches, especially artificial neural networks, very significantly improve thermal performance assessment in building envelopes regarding accuracy and efficiency.

The integration of Infra-Red thermography (IRT) and photogrammetry in the inspection of building envelopes is studied by using this article "UAS IR-Thermograms Processing and Photogrammetry of Thermal Images for the Inspection of Building Envelopes" [44]. The research highlights the fact that the combination of thermal images captured by Unmanned Aerial Systems (UAS) with advanced photogrammetric software enhances the data analysis and interpretation process in identifying structural anomalies without contact and will improve such accuracy and efficiency in future.

The [48] article under the title "Building Condition Ratings by Applying Infrared Thermography: A Preliminary Study" defines the Non-Destructive Testing (NDT) category of infrared thermography, which is used to detect building defects owing to cracks, water penetration, dampness, as well as structural irregularities. This study mentions that there is good improvement brought in by the incorporation of IRT because it is combined with conventional visual inspections. The authors eventually mention about footnoting extensive research into the validation of the use of IRT in building

diagnostics, but say that his usage, when combined with visible inspections, scales better and is more accurate in interpreting large datasets of thermal images.

The work [48] proposed a multiscale analysis of thermographic data by means of a combination of Multidimensional Empirical Mode Decomposition (MEEMD) and Principal Component Analysis (PCA). MEEMD decomposes thermographic images into different spatial scales, thus enabling the separation of structural information from noise and thermal backgrounds. The next step is to apply PCA toward the discovery of the most significant features in the data for compressing information and emphasizing the most meaningful structures. Such theoretical ground was demonstrated experimentally in the testing of concrete walls, within which a higher accuracy was achieved by detecting structures like sealed doors and slabs. While the methodology is highly complex, it works away subjectivity by completely relying on well-defined mathematical principles. However, detection analysis may be automated by programming techniques for human operationalizing purposes. This brings various advantages: it reduces human error, ensures consistent evaluation and allows processing on a large scale with little to no manual intervention. In addition, when a complete framework is integrated with machine learning techniques, it would further enable continuous refinement of automated models and improvement of their prediction over time. While cost and operation could be drawbacks, strides in optimization and hardware enable ever quicker and scalable thermographic analyzed solutions.

The study, "Performance Comparison of Several Deep Learning-Based Object Detection Algorithms Utilizing Thermal Images" [49] assesses six deep learning algorithms in terms of their ability to detect objects using thermal images: SSD, ResNet, MobileNet, EfficientDet, Faster R-CNN, and YOLO. The dataset consisted of only 56 images, therefore, the transfer learning process applied pre-trained models. Results indicated that EfficientDet recorded the highest accuracy and classification loss, followed by Faster R-CNN. Hence, it can be inferred from the abovementioned findings that EfficientDet is the most suitable algorithm for thermal image object detection, and Faster R-CNN provides satisfactory results. It illustrates the application of passive IRT for diagnosing building pathologies and evaluating the thermal performance of facades in Coimbra, Portugal. By performing a thermal inspection with a camera mounted on a drone, the study aspires to ease the inspection of high-rise and inaccessible edifices. It is meant to diminish intrusiveness and accelerate data collection. According to the authors, while aerial

thermography is efficient, it has a major disadvantage: noise is higher in thermal images due to excess features of the urban landscape, making interpretation quite hard. Therefore, it would be helpful to have an automatic system that segments out the relevant area and pulls out the temperature data needed to greatly improve accuracy and speed the analysis.

The paper "Occupancy Estimation Using Thermal Imaging Sensors and Machine Learning Algorithms" [54] discusses occupancy estimation in smart buildings using low-resolution thermal imaging sensors in combination with machine learning techniques. This non-invasive method may serve security, surveillance, traffic management, and resource optimization endeavors. Three thermal imaging sensors were examined for different resolution characteristics with emphasis on sensing characterization and accuracy on occupancy estimation. A standard algorithm processing pipeline is proposed for occupancy estimation, comparing the results from the three sensors, which confirms that low-resolution thermal imaging sensors can estimate occupancy in real time with high efficacy despite their poor resolution. Hence, it further establishes the capability of integrated solutions for accurate real-time occupancy estimation using thermal imaging sensors and machine learning algorithms in smart buildings, which in turn serve as a non-intrusive solution to operational efficiency in monitoring and management of occupancy in buildings.

"Machine Learning Models Applied to Moisture Assessment in Building Materials" [55] discusses how artificial neural networks (ANNs) were used for predicting moisture content in building materials from the surface temperature. The non-destructive measuring method greatly enhances accuracy and efficiency in the assessment of moisture, which can be followed by evaluating the thermal performance of the buildings. Surface temperature and moisture content information from different building materials were gathered to train the ANN model using supervised learning. The results proved that the ANN predicted moisture content with higher accuracy and better speed than traditional methods. Nonetheless, for effective application, a good amount of data would need to be collected, and model training and validation would have to be attained to obtain accuracy and generalize the findings. In conclusion, this study suggests that there is potential to combine machine learning with infrared thermography for accurate and non-destructive evaluation of moisture in buildings, thereby increasing the efficiencies of these diagnostics and aiding the decision-making process.

Findings [56] showed that the older brick buildings are more prone to retain moisture, thus aggravating thermal anomalies and energy losses. The result casts prospects for undertaking quantitative thermal analysis to refine automated defect identification in IRT applications. Using the temperature index (TI) method and image subtraction techniques, quantification of leakage severity and enhancement of thermal pattern detection have been done. The revealed results validated IRT in locating air infiltration points, especially around window frames and joints, but analysis is operator-dependent; hence, automation is deemed necessary.

In [57], infrared thermography (IRT) is suggested as an assessment method for thermal defects in building envelopes, focusing on the Improved Temperature Factor (ITF) framework and moisture analysis. ITF refinement by using mean temperature factors (fRs), maximum (fMs), and minimum (fms) temperature factors has allowed for finer evaluations of thermal defects due to conduction, which are influenced by wall orientation and structural amendment. Moisture was diagnosed to exist as either capillary rise, moisture that was retained internally, or moisture that was infiltrated externally; with fms being the principal variable, since it dampened the cooling effect due to moisture.

A newly proposed method for evaluating the thermal transmittance (U-value) of building envelopes using thermal imaging and machine learning is given in the paper titled "Estimating Surface Temperature from Thermal Imagery of Buildings for Accurate Thermal Transmittance (U-value): A Machine Learning Perspective" [58]. The authors proposed a three-layer framework that processes thermal images of a building structure to be captured by Unmanned Aerial Systems (UAS) and relate this information to estimates of surface temperature to improve accuracy, thus enhancing U-value calculations, particularly critical to energy efficiency assessment. Over 100,000 augmented thermal images from multiple campus buildings were used in this study. This study casts a glimpse of the capabilities of machine learning to conjure in automating thermal image analysis to assess building performance with a more effective and accurate alternative to U-value computation methods already in use.

3. METODOLOGY

This chapter describes the methodology applied to develop and validate software for the automatic detection of construction pathologies using thermal images. The methodological process was structured sequentially (Figure 11) and divided into six main stages: problem definition, image database construction, software development, image calibration and preprocessing, anomaly detection, and data export.



Figure 11- Flow chart of the program.



Figure 11- Flow chart of the program.

3.1. Problem definition

The analysis of thermal images for building diagnostics is traditionally performed manually and requires specialized technical expertise. This process is prone to interpretive variability, low standardization, and scalability issues, especially when handling large datasets. To mitigate these limitations, this research proposes the development of a computational tool for the automatic detection of construction pathologies based on thermal image processing.

3.2. The database

The tool was tested using 16 reference thermal images, from previous research [59], in which a database of thermal images was created illustrating two different cases of humidification: partial humidification by the lower face of a concrete specimen and another by the upper face. Each image was treated as a test case for functional validation of the software. Although the database is limited, its selection included thermal and structural variations relevant to the identification of pathological patterns.

3.3. Software development

The software is developed using the Python programming language, with the assistance of Pygame libraries for the graphical user interface and OpenCV for image processing. Other libraries were used, like NumPy, Matplotlib and Tkinter.

- **OpenCV**: for image processing and analysis;
- **NumPy**: for matrix operations and numerical processing;
- **Pygame**: for the creation of the graphical interface;
- **Tkinter**: for GUI window interactions;
- **Matplotlib**: for the generation of custom colormaps.

The software allows the import and processing of images in various formats, including JPG, PNG, RAW, IS2, among others. The functionalities have been organized into three main modules:

- Graphical interface: allows interaction with the user and visualization of results.
- Image processing: application of filters, thermal segmentation, calibration and statistical analysis.
- Data export: allows you to save processed images and thermal matrices in formats compatible with external analysis (CSV, PNG).

The core technique employed is thermal image analysis, aiming to maximize anomaly detection and area of interest segmentation. For this purpose, image processing filters such as the Gaussian filter, the Median filter, and the Bilateral filter were utilized. Additionally, the software supports segmentation with temperature ranges, dividing the picture into areas defined by user-specified temperature ranges, in addition to potential anomaly detection based on statistical calculations such as percentile analysis to identify significant changes in temperatures. The software allowed the analysis of thermal images in different file formats, focusing on hot and cold spot detection, thermal data temperature calibration, and the export of thermal data in CSV format.

The thermal image processing system represents an advanced computational solution for the analysis and manipulation of thermographic data. Developed entirely in Python, the application offers a graphical interface rich in functionality, allowing users to perform complex operations of treatment and visualization of thermal images. In it is possible to see the program's flowchart showing the processes, from its initialization, through image processing to image export.

3.4. Calibration and pre-processing

The main functionalities of the system are described below, according to their order of application:

- Noise removal: application of filters (median, gaussian, bilateral) to reduce thermal artifacts that may affect the reading.
- Temperature calibration: adjustment of the thermal scale based on minimum and maximum values informed, ensuring consistency with the real image data.
- Definition of the analysis area: allows you to manually delimit regions of interest within the image to focus segmentation and reduce interference from irrelevant areas.
- Thermal range segmentation: divides the image into user-defined temperature ranges, facilitating the identification of critical zones.
- Detection of anomalies by percentile: automatically identifies regions whose temperature is below a statistical threshold (e.g. 5th percentile), associated with humidity or construction flaws.
- Color detection: complementary analysis that highlights areas with abnormal chromatic variation, useful for reinforcing the identification of thermal patterns.

3.5. Anomalie detection

The anomaly detection module plays a central role in the system's ability to identify thermal patterns associated with pathologies. Users can choose between two detection strategies:

- **Percentile-based detection:** Automatically highlights temperature values in the highest or lowest percentiles (e.g., top 5%), based on statistical distribution. This is useful for identifying outliers that may indicate thermal bridges, moisture, or detachment of surface layers.
- **Color-based detection:** Enables the user to select specific colors or temperature ranges to be detected based on the segmented thermal image. This method offers more visual control and is useful when the user has prior knowledge of the expected anomaly temperature ranges.

Once the detection method is selected, the system processes the entire image or a manually defined region of interest (ROI). Detected areas are highlighted directly on the thermal image and exported along with the CSV temperature matrix.

The anomaly detection module was designed to be flexible and intuitive, supporting both exploratory analysis and repeatable diagnostics across multiple images.

3.6. Data export

The data of the processed images can be exported in two formats:

- Image with markings: visualization with the anomalous areas highlighted.
- Thermal matrix: export of all temperature values in CSV for later statistical analysis.

3.7. Justification of the approach

In the initial stages of this research, the implementation of convolutional neural networks (CNNs), particularly the YOLOv7 architecture, was considered as a potential strategy for the automated detection of anomalies in thermal images. Such models are widely recognized for their effectiveness in object detection and classification tasks, especially when applied to large-scale datasets. However, the available dataset in this study consisted of only 16 thermal images, which are insufficient for the training, validation, and testing processes required by deep learning algorithms. As a result, this approach was deemed impractical given the limited data and the potential risk of overfitting and poor generalization.

Considering these constraints, a rule-based methodology was adopted, employing segmentation by temperature intervals and anomaly detection based on statistical percentiles. Although these techniques are comparatively simpler, they offer robustness and interpretability, particularly in contexts where data availability is restricted. Moreover, they allow for consistent identification of thermal irregularities associated with construction pathologies, such as moisture infiltration or thermal bridging, without the need for extensive computational resources.

The software developed in this work was intentionally designed to be lightweight, accessible, and intuitive, with a graphical user interface tailored for professionals in the field of building diagnostics who may not possess programming expertise. This usability-focused design influenced the selection of algorithms and functionalities, prioritizing clarity and efficiency over algorithmic complexity.

Despite its operational advantages, the proposed approach presents some limitations:

- **Limited dataset size:** the small number of reference images restricted the statistical validation of the results and prevented the use of data-intensive models.
- **Lack of empirical validation:** no direct comparison was made between the tool's outputs and in-situ inspection results, which constrains the assessment of real-world accuracy.
- **Restricted generalizability:** the system may not perform optimally when applied to images captured under different environmental conditions or using different equipment.
- **Absence of sensor integration:** the software currently supports only static image input and does not include real-time data acquisition or communication with thermal imaging devices.

3.8. Program implementation

3.8.1. Key features

3.8.1.1. Image Upload

The program supports several types of image files for reading and subsequent processing. The supported formats include:

- BitMaP (BMP).
- Pickle Format (PKL).
- Joint Photographic Experts Group (JPG/JPEG).
- Portable Network Graphics (PNG).
- Tag Image File Format (TIFF).
- Graphics Interchange Format (GIF).
- Unprocessed Data (RAW).
- Intelligence Specialist Petty Officer 2nd Class (IS2).
- Exchangeable Image File Format (EXIF).

To upload an image, it is necessary to follow a series of steps. Upon initiating the program, users are presented with the option to select the image for analysis from the supported formats. Once a single image has been chosen, the user must click the "Open" button located in the lower right corner, as illustrated in Figure 12. Additionally, the user may adjust the file type filter to "All supported files" in the same lower right corner,

facilitating the location of different file types. The program will then automatically resize proportionally the selected image to 640 x 512 pixels for optimal analysis.

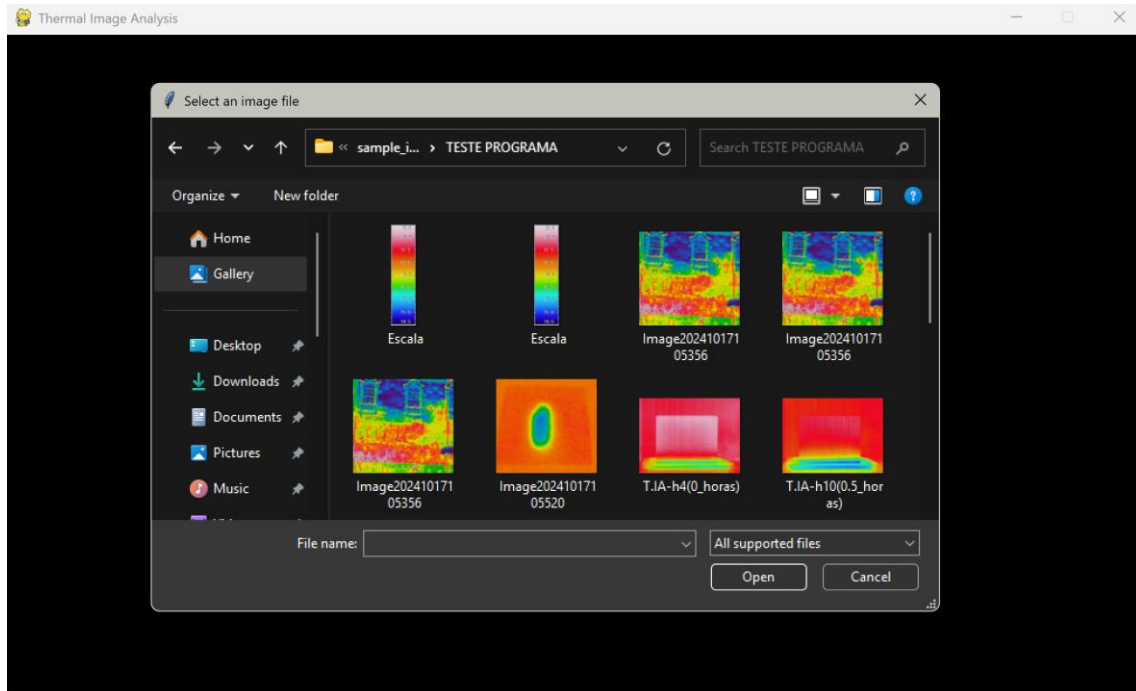


Figure 12- Window of the startup of the program.

3.8.1.2. Image processing

The processing of thermal images is a critical step in the analytical workflow, as it enhances image quality and prepares the data for subsequent analysis. The program employs four distinct approaches: noise filters, which utilize median filters to remove salt-and-pepper noise, Gaussian filters, to smooth the image while preserving edges, bilateral filters, to maintain sharp transitions in temperature while reducing noise in homogeneous regions, and colormaps, which are used to visualize the temperature distribution within the image. These techniques enable the user to conduct a comprehensive and efficient analysis of the thermal images, contributing to the generation of accurate and interpretable results.

The “*remove_noise*” function, presented in Figure 13, illustrates this approach.

```

def remove_noise(self):
    """
    Removes thermal image noise by correcting low-temperature outliers
    surrounded by high temperatures and applying smoothing filters.
    """
    if not hasattr(self, 'mat'):
        self.show_message("Upload an image first!")
        return

    # Creates a copy of the temperature matrix to work with
    mat = self.mat.copy()

    # Sets a threshold to identify outliers
    # A point is considered an outlier if it is much colder than its
neighbors
    threshold = 0.1 # Adjust this value as needed

    # Iterates over each pixel of the image
    for y in range(1, mat.shape[0] - 1):
        for x in range(1, mat.shape[1] - 1):
            # Gets the value of the current pixel and its neighbors
            current_temp = mat[y, x]
            neighbors = [
                mat[y - 1, x], # Neighbor above
                mat[y + 1, x], # Neighbor below
                mat[y, x - 1], # Neighbor on the left
                mat[y, x + 1], # Neighbor on the right
                mat[y - 1, x - 1], # Upper left diagonal neighbor
                mat[y - 1, x + 1], # Upper right diagonal neighbor
                mat[y + 1, x - 1], # Lower left diagonal neighbor
                mat[y + 1, x + 1], # Lower right diagonal neighbor
            ]

            # Averages neighbors
            mean_neighbors = np.mean(neighbors)

            # Check if the current pixel is outlier
            if current_temp < (mean_neighbors - threshold):
                # Replaces the pixel value with the average of the
neighbors
                mat[y, x] = mean_neighbors

    # Applies a median filter to smooth the image
    mat = median_filter(mat, size=40)

```

Figure 13- Remove Noise function

The “*apply_color_map*” function is detailed in Figure 14.

```

def apply_color_map(self, colorMap):
    if not hasattr(self, 'mat') or self.mat is None:
        return

    # Normalize the temperature values
    norm = colors.Normalize(vmin=self.meta["min_temp"],
vmax=self.meta["max_temp"])
    cmap = colormaps.get_cmap(colorMap)

    # Apply the colormap to the thermal data
    mapped_data = cmap(norm(self.mat))

    # Convert to an RGB image (ignoring the alpha channel)
    self.rgb_image = (mapped_data[:, :, :3] * 255).astype(np.uint8)

    # Update the display
    self.apply_color_map(self.colorMap)

```

Figure 14- Apply Color Map function

3.8.1.3. Temperature Calibration

After image processing, another crucial step in the analysis is temperature calibration. This ensures that the displayed temperature values of the image match the actual measured values, calibrating the temperature variation. For the anomaly detection and temperature segmentation, this process is indispensable for precise and reliable results, if not made can lead to an inaccurate conclusion about the area analyzed.

The user can access this functionality just after loading a thermal image, in the menu on the left side of the window (Figure 15). The user must click the "*Calibrate Temperature*" button located in the program interface. This action opens a new window or section where the user can input the minimum and maximum temperature values that correspond to the loaded thermal image. These values can be obtained from known measurements or the specifications of the equipment used to capture the image. The interface provides input fields for these values, facilitating precise entry (Figure 16). The temperature scale on the right side of the interface will change after the calibration as shown in the Figure 17. The user will be able to see the temperature also when moving the mouse through the image and can then know the specific temperature value of each pixel (Figure 18).

After entering the values, the user must click the "*Apply Calibration*" button. The system will adjust the temperature scale of the image, for the values provided, establishing that subsequent analysis is going to be accurate.

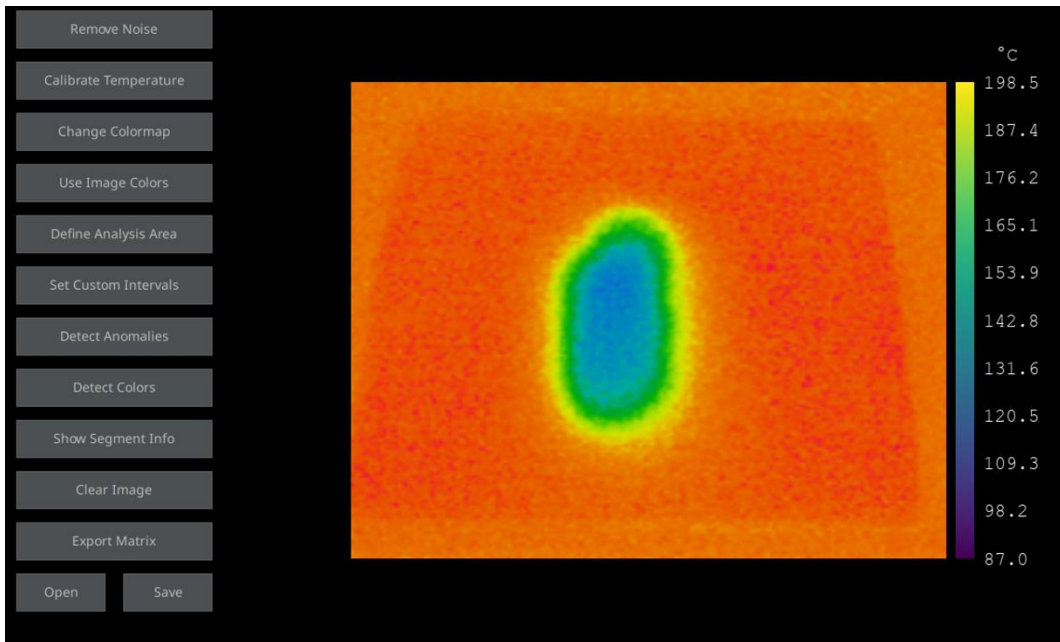


Figure 15- Home of the program before calibration.

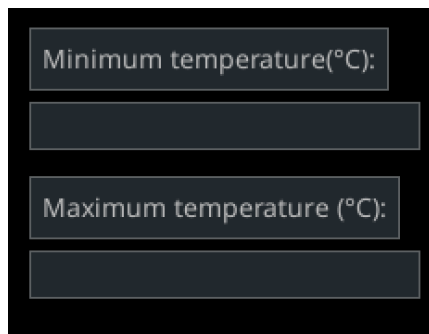


Figure 16- Menu of the calibrate temperature.

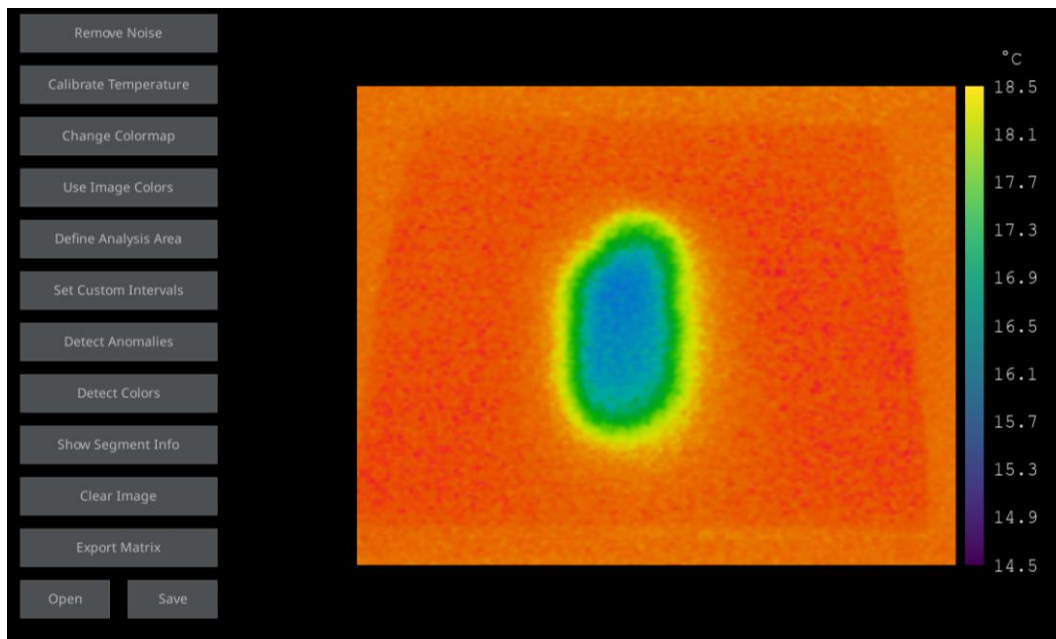


Figure 17- Home of the program after calibration.

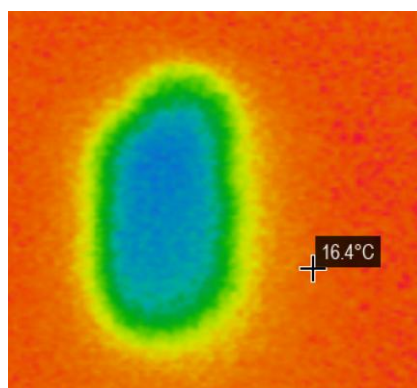


Figure 18- Temperature of the pixel.

3.8.1.4. Colormap

In this section of the program, a function called Colormap (filters) is used to map numerical values, such as temperatures, intensities, or scalar data, to corresponding colors. It transforms numbers into visible colors, allowing for intuitive data visualization. The colormap in thermal images is used to represent different temperatures with distinct colors, these colors can be used in two ways: with predefined colors and by creating colors from the image itself. The program uses both modes and adjusts the color and temperature scales when they are being applied.

The colormaps that are predefined tend to work better with black and white images, and can be used by clicking the "Change Colormap" button. For colored images, it is recommended to use the "Use Image Colors" button. The colormaps included in the

program, along with their advantages, disadvantages and recommend uses, are detailed below:

- **Plasma** (Figure 19)

Advantages:

- Perceptually uniform: the color variation is consistent with the data variation.
- Vibrant colors: the transitions between purple and orange are visually appealing.
- Good contrast: it helps identify subtle variations in the data.

Disadvantages:

- Dark colors: it can be difficult to distinguish variations in regions with very dark colors.

Recommended Use:

- Scientific visualizations and data with subtle variations.

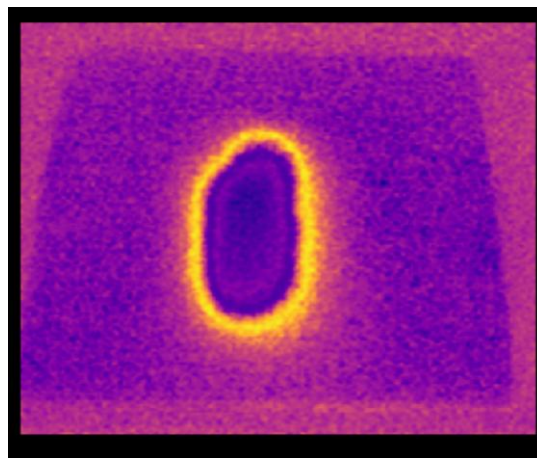


Figure 19- Colors of plasma.

- **Inferno** (Figure 20)

Advantages:

- Perceptually uniform: the color variation is consistent with the data variation.
- High contrast: ideal for highlighting extreme variations in the data.
- Good for high-contrast data: it helps identify high and low values.

Disadvantages:

- Dark colors: it can be difficult to distinguish variations in regions with very dark colors.

Recommended Use:

- High-contrast data, such as extreme temperature variations.

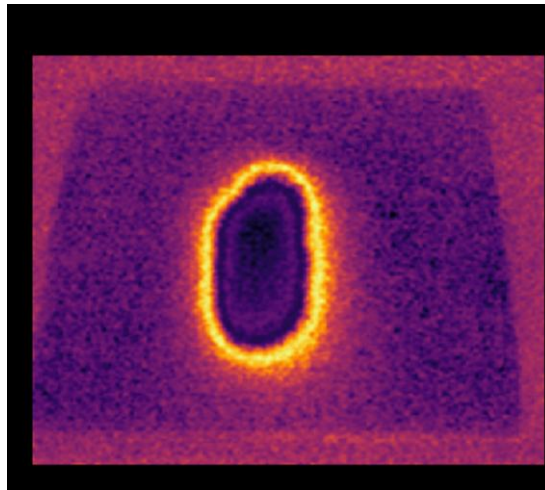


Figure 20- Colors of inferno.

- **Magma**(Figure 21)

Advantages:

- Perceptually uniform: the color variation is consistent with the data variation.
- Smooth transitions: the colors range from black to purple, orange, and white, creating a smooth transition.
- Good for high-contrast data: it helps identify high and low values.

Disadvantages:

- Dark colors: it can be difficult to distinguish variations in regions with very dark colors.

Recommended Use:

- High-contrast data and scientific visualizations.

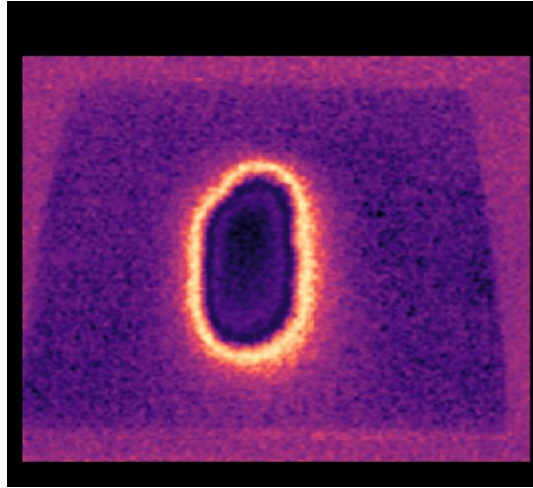


Figure 21- Colors of magma.

- **Cividis** (Figure 22)

Advantages:

- Perceptually uniform: the color variation is consistent with the data variation.
- Suitable for color blindness: it makes it easier for people with color blindness to distinguish the colors.
- Good for quantitative data: ideal for modern scientific visualizations.

Disadvantages:

- Less vibrant colors: compared to Jet, the colors may seem less striking to some users.

Recommended Use:

- Quantitative data and scientific visualizations.

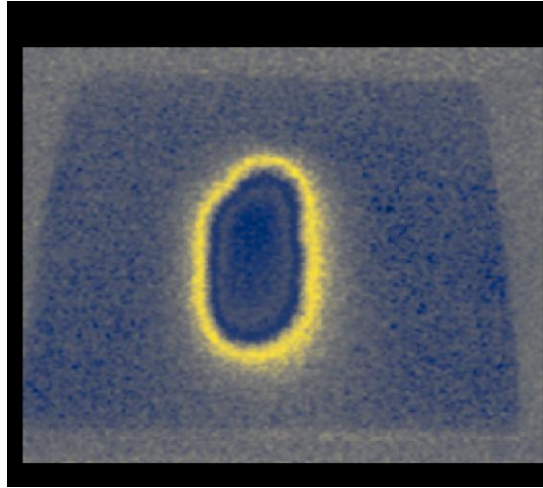


Figure 22- Colors of cividis.

- **Coolwarm** (Figure 23)

Advantages:

- Divergent: ideal for data that has an important central point (such as zero).
- Good contrast: it helps identify positive and negative values.
- Intuitive colors: blue (cold) and red (hot) are intuitive for representing extremes.

Disadvantages:

- Not sequential: not ideal for data that varies only from low to high.

Recommended Use:

- Data with positive and negative values, such as temperature deviations.

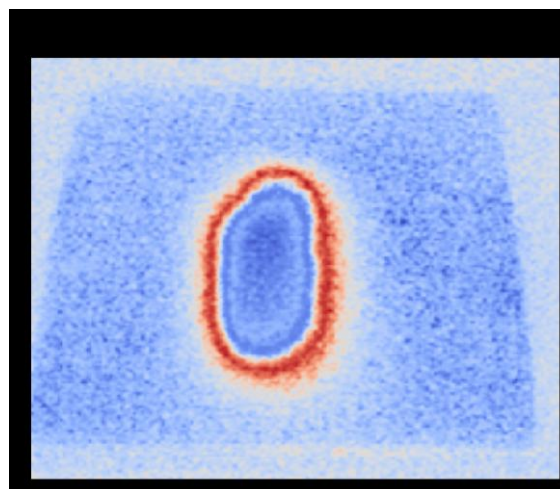


Figure 23- Colors of coolwarm.

- **Spring** (Figure 24)

Advantages:

- Vibrant colors: the transitions between magenta and yellow are visually striking.
- Good for highlighting variations: it helps identify variations in the data.

Disadvantages:

- Not perceptually uniform: the color variation does not consistently reflect the data variation.
- Very saturated colors: it can be tiring for prolonged visualizations.

Recommended Use:

- Visualizations that need vibrant and striking colors.

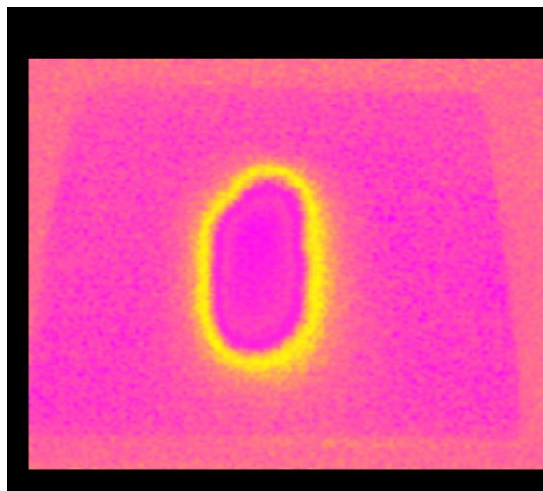


Figure 24- Colors of spring.

- **Autumn** (Figure 25)

Advantages:

- Warm tones: the colors red and yellow are ideal for representing warm data.
- Good for highlighting variations: it helps identify variations in the data.

Disadvantages:

- Not perceptually uniform: the color variation does not consistently reflect the data variation.

- Limited colors: only shades of red and yellow may not be ideal for all types of data.

Recommended Use:

- Visualizations that need warm tones, such as temperature variations in warm environments.

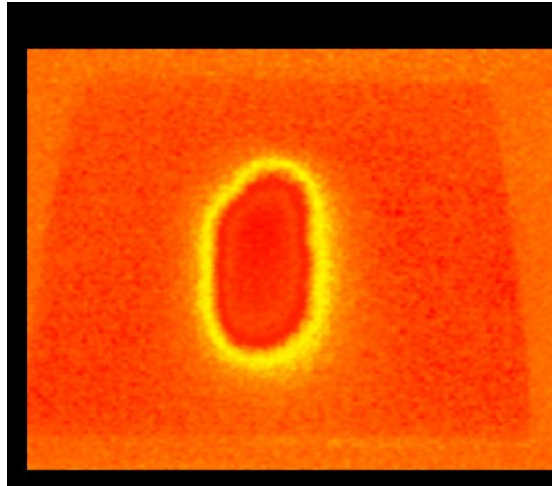


Figure 25- Colors of autumn.

- **Jet** (Figure 26)

Advantages:

- Immediate recognition: it is a classic and widely used colormap, so many people are familiar with it.
- Vibrant colors: the transitions between blue, green, yellow, and red are visually striking.

Disadvantages:

- Not perceptually uniform: the color variation does not consistently reflect the data variation. This can lead to misinterpretation of the data.
- Color blindness issues: it makes it difficult for people with color blindness to distinguish the colors.
- Incorrect highlighting: intermediate values (green and yellow) can appear more important than they are.

Recommended Use:

- Classic visualizations but should be avoided for quantitative data.

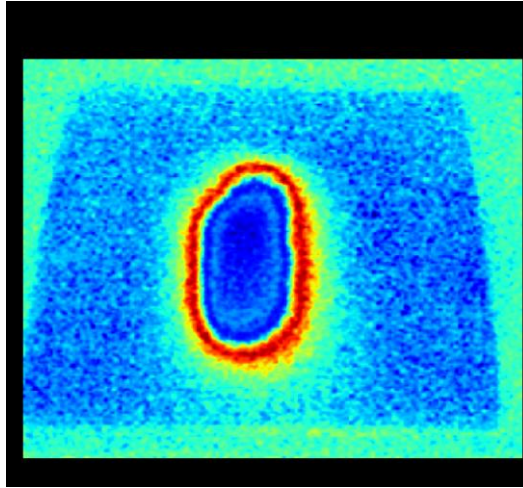


Figure 26-Colors of jet.

- **Viridis** (Figure 27)

Advantages:

- Perceptual uniform: the color variation consistently reflects the data variation.
- Suitable for color blindness: it makes it easier for people with color blindness to distinguish the colors.
- Good for quantitative data: ideal for modern scientific visualizations.

Disadvantages:

- Less vibrant colors: compared to Jet, the colors may seem less striking to some users.

Recommended Use:

- Quantitative data, such as temperatures or continuous variations.

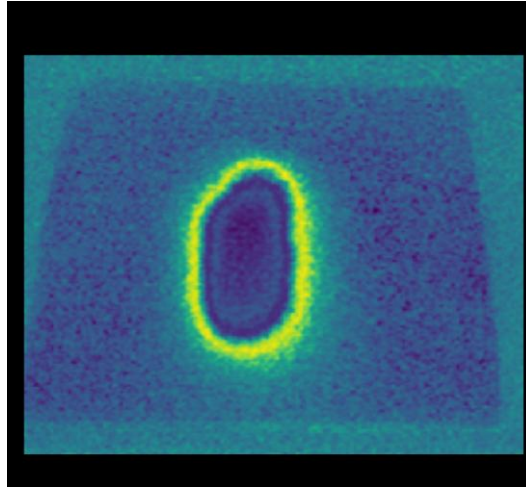


Figure 27- Colors of Viridis.

The software offers two options for viewing the colors of the image: the application of custom colormaps (such as *inferno*, *viridis*, among others) or the preservation of the original colors of the thermal image provided by the user. When the second alternative is chosen, the coloration is maintained **based on loaded image**, allowing the thermal analysis to respect the visual scale used at the time of capture.

- **Based on Loaded Image**

- Extracts unique colors from the image.
- Sorts the colors by hue in the HSV color space.
- Creates a gradient with sorted colors.
- Returns a custom colormap that can be applied to the image.

Advantages

- The custom colormap reflects the real colors of the image, which can be more intuitive for the user.
- If the image already has significant colors (e.g., a thermal photograph with specific colors for temperatures), the custom colormap preserves this familiarity.
- The color bar and the image will have the same color palette, creating a more cohesive visual experience.

- This is especially useful when the image already has a specific aesthetic you want to maintain.
- The colormap is generated based on the unique colors of the image, which means it is specifically tailored for that image.
- This can highlight unique features of the image that a predefined colormap would not.
- If the original image is already colored (e.g., an RGB photograph), the custom colormap preserves these colors instead of replacing them with an artificial gradient.

Disadvantages

- The custom colormap may not consistently reflect data variation. For example, two close temperatures might be represented by very different colors, or vice versa.
- This can make data interpretation difficult, especially in scientific or quantitative applications.
- If you are comparing multiple images, each with its own custom colormap, it can be hard to establish a direct relationship between colors and data values.
- Predefined colormaps (like Viridis or Plasma) are more consistent and allow direct comparisons.
- The custom colormap may not be suitable for people with colorblindness, especially if the image colors are not chosen with this in mind.
- Colormaps like Viridis or Cividis are designed to be perceptually uniform and accessible.
- If the original image has little color variation or very similar colors, the custom colormap may not effectively highlight data variations.
- Predefined colormaps are designed to maximize contrast and distinction between values.
- Creating and applying a custom colormap requires more processing and can be more complex to implement than using a predefined colormap.

Recommended Use:

- If the image already has colors that represent something specific (e.g., colors indicating temperatures or regions of interest), the custom colormap may be the best choice.
- When the visual appearance of the image is more important than quantitative accuracy (e.g., in presentations or visual reports).
- When you want to maintain the original colors of the image without applying an artificial gradient.

3.8.1.5. Definition of the Analysis Area

Defining an area of analysis is a critical step to ensure a more accurate and precise evaluation of the image. By concentrating the analysis on specific or smaller regions, the user can focus on the relevant areas while disregarding irrelevant sections. This approach allows for a more detailed and precise analysis, enabling the identification of temperature variations that might otherwise be overlooked in a broader examination.

The user can use this function by clicking the "*Define Analysis Area*" button in the program menu. Then, the user should click and drag the mouse over the thermal image to select the area of interest. The selected area will be highlighted with a border and a mask, visually indicating the region that will be analyzed (Figure 28).

After selecting the area, the user can adjust and edit the size and position of the box that was created by dragging the borders or the content of the selection or dragging the whole box. This procedure allows refining the analysis area and guarantees that the box covers the entire region of interest.

Once the analysis area is defined, the user can continue with the analysis by temperature segmentation, or anomaly detection within this specific area.

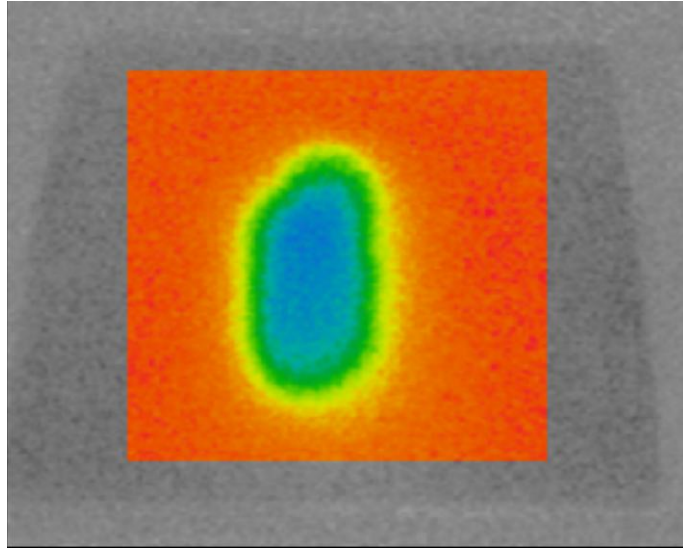


Figure 28- Definition of the area of analysis.

3.8.1.6. Temperature Segmentation

Temperature segmentation is employed in thermal imaging to divide the image into distinct regions, based on either predefined or customized temperature ranges. The function first calculates the temperature intervals and then creates a mask for each interval. This method facilitates the visualization of different regions within the thermal image, allowing for a clearer understanding of temperature distribution.

Segmentation is performed using the “*auto_segment*” function presented in Figure 29.

```

def auto_segment(self):
    if self.analysis_area:
        x, y, w, h = self.analysis_area
        data = self.mat[y:y+h, x:x+w]
        offset = (x, y)
    else:
        data = self.mat
        offset = (0, 0)

    min_temp = np.floor(np.min(data))
    max_temp = np.ceil(np.max(data))
    num_intervals = int(max_temp - min_temp) + 1
    intervals = np.linspace(min_temp, max_temp, num_intervals)

    segments = ThermalAnalysis.auto_segment(data, intervals)

    # Adjust masks for the correct position in the full image
    if offset != (0, 0):
        adjusted_segments = {}
        for temp_range, segment in segments.items():
            full_mask = np.zeros_like(self.mat, dtype=bool)
            full_mask[y:y+h, x:x+w] = segment['mask']
            segment['mask'] = full_mask
            adjusted_segments[temp_range] = segment
        segments = adjusted_segments

    self.segments = segments
    self.update_segment_overlay()
    self.show_message(f"Auto-segmented into {len(segments)} intervals")

```

Figure 29- Auto Segment function.

After defining the area of the analysis, the temperature range can be set using the “Set custom intervals” button. A specific menu for that purpose will open (Figure 30), allowing the user to enter the minimum and maximum temperatures to be analyzed. During the segmentation step, the temperature range is divided into intervals, determining which segments will be displayed in relation to the selected analysis range. After setting these parameters, the temperature intervals will be shown in different colors. The defined temperature ranges will be represented using colors in the image, while areas with temperatures outside these ranges will appear in grayscale (Figure 31).

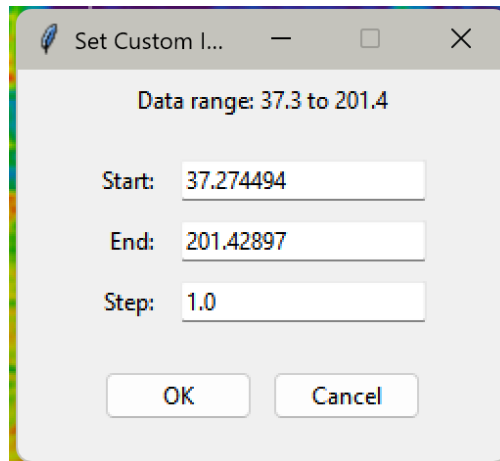


Figure 30- Menu of the Set Custom Range.

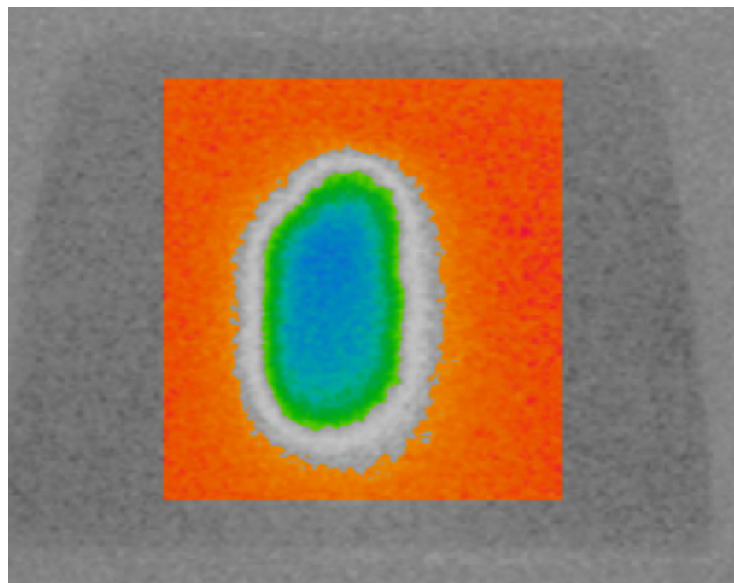


Figure 31- Image after the definition of the interval and number of steps.

3.8.1.7. Anomalies detection

Despite the provision in the software for manually choosing the temperature range from a manual selection, a specific feature known as "*Detect Anomalies*" has been added so that automatic detection of thermal anomalies can be possible. It is an important component of the software because it enhances the performance in thermal image analysis by automatically finding areas where temperatures vary significantly from what is anticipated within the range. Statistical percentile analysis is utilized in detecting anomalies to increase the precise the coldest points of the thermal image. The user can choose the percentile value as depicted in Figure 32.

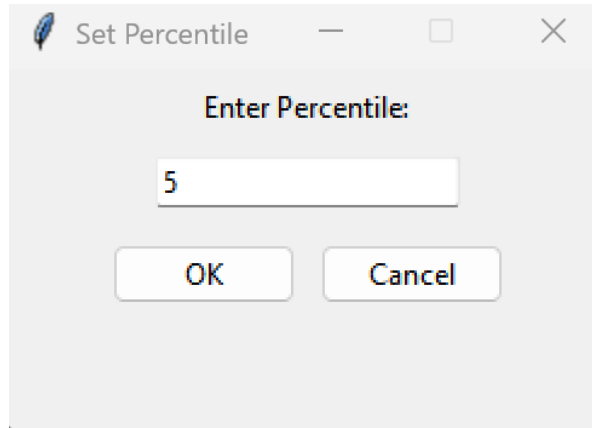


Figure 32- Definition of the percentile for anomalies detection

The percentile of the temperature distribution is first calculated within the defined analysis area or across the entire image. This percentile is then used as a threshold to identify the coldest regions, i.e., the data points that fall below this value. This process is illustrated:

$$threshold = P_{percentile}(T) \quad (1)$$

Where:

- $P_{percentile}$ is the percentile function.
- T is the set of thermal data.

And the for the mask the equation used was:

$$mask(x, y) = \begin{cases} \mathbf{True} & \text{if } T(x, y) \leq threshold \\ \mathbf{False} & \text{otherwise} \end{cases} \quad (2)$$

Where:

- $T(x, y)$ is the temperature value at pixel (x, y) .
- $threshold$ is the temperature value calculated based on the percentile.

The software subsequently scans the image pixel by pixel, picking up areas in which the temperature falls below this specified level. Such areas are referred to as possible anomalies because they are discrepant from those of most of the image. This automated process not only enhances the efficiency of the analysis process but also minimizes the possibility of human error, thereby making the process consistent and reliable. The software offers a strong platform for thermal anomaly detection using percentile-based statistical approaches, which is highly suited to predictive maintenance, quality control,

and structural diagnostics applications. A white mask is applied in this case, to show a contrast with the rest of the thermal image (Figure 33).

This button is also compatible with the “*Define Analysis Area*” one, which displays results exclusively for the specified area, utilizing only the temperature data defined within that area for calculations (Figure 34).

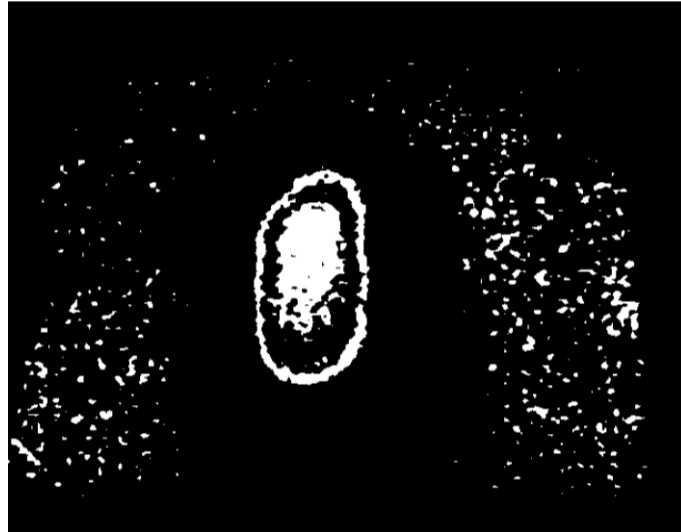


Figure 33- Detect possible anomalies using percentile function.

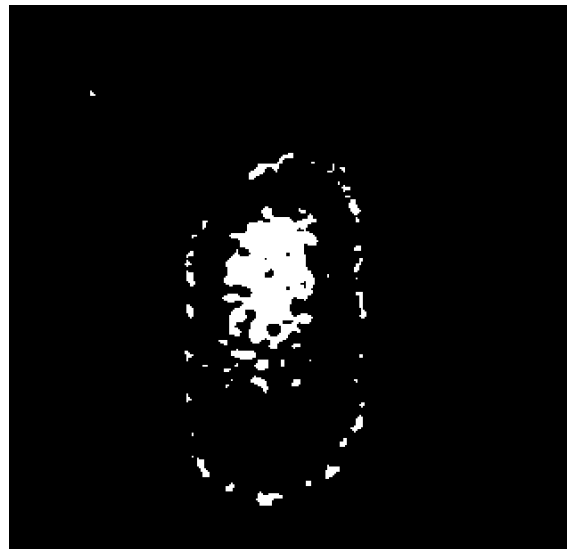


Figure 34- Detect possible anomalies in a defined area.

In addition to thermal anomaly detection, the program also includes a color-based detection feature, implemented using the OpenCV library, available in the button “*Detect Colors*”. This functionality aims to identify specific areas in the image based on their color properties, providing an additional layer of analysis. The color detection process is particularly useful for highlighting regions with distinct color patterns, which may

correspond to specific materials, defects, or anomalies. The image in this case shows up in another window, with “black and white” theme, the white part of the image is the called “anomalies” (Figure 35). This button is compatible with the “*Define Analysis Area*”, which displays results exclusively for the specified area (Figure 36).

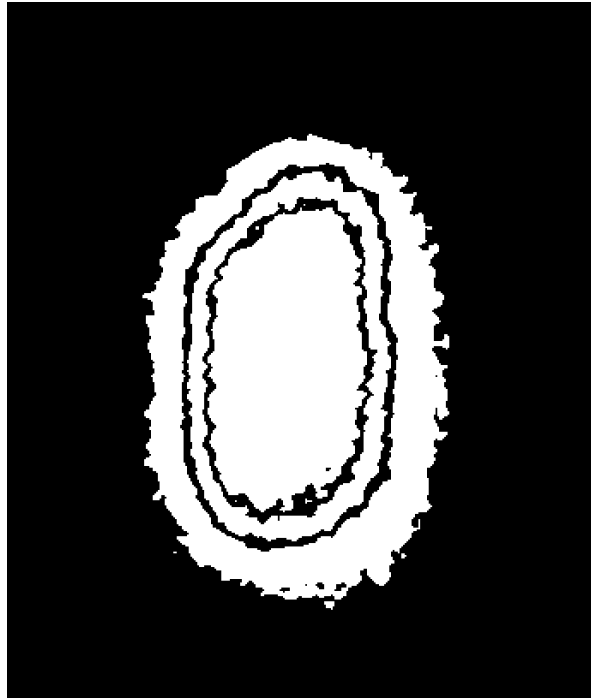


Figure 35- Detection using colors patterns.



Figure 36- Detection using colors patterns only in a specific area of the image.

3.8.1.8. Clear Image

In the program, there is also a "*Clear Image*" button that allows users to clear the image of all the applied parameters. When clicking the button, a new menu will open, where you can choose what you want to clear (Figure 37). To return to the previous menu, simply click the "Back" button.

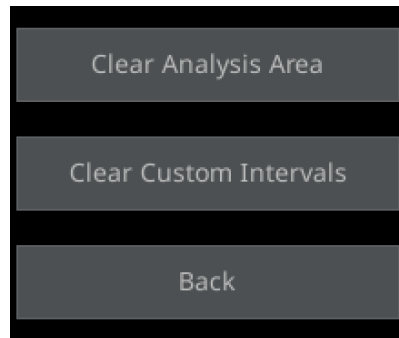


Figure 37- Clear image menu.

3.8.1.9. Segment Info

The program has the option to display information about the selected temperature range in item 3.1.1.6. In the "*Show Segment Info*", for each segment, the percentage of the total image area that the segment covers are calculated (Figure 38). If an area of analysis is defined, the program will also calculate the percentage of the area covered by the segment. This information is compiled into a formatted string that is displayed in the segment information window. The compiled segment information is presented in a text box within the segment information window. This includes details such as temperature range, percentage of the total and area of analysis covered, pixel count, average temperature, and standard deviation. If an analysis area is defined, additional statistical information about the analysis area (such as minimum, maximum, mean, and median temperatures) will also be displayed. The user can view this information to understand the distribution and characteristics of different temperature segments in the image. This can be useful for identifying areas of interest or possible anomalies in the thermal data.

```

Temperature Segment Information:
-----
Temperature Range | Area (px) | % Total | Avg Temp (°C) | Std Dev (°C)
-----
No temperature segments defined.

Information of Color-Detected Areas:
-----
Color | Area (px) | % Total | Min Temp (°C) | Max Temp (°C) | Avg Temp (°C)
-----
Blue | 0 | 0.00% | 0.00 | 0.00 | 0.00
Green | 7726 | 2.36% | 148.00 | 158.21 | 151.05
Cyan | 4796 | 1.46% | 158.79 | 175.00 | 164.36
Yellow | 17015 | 5.19% | 157.41 | 195.00 | 180.97
Purple | 0 | 0.00% | 0.00 | 0.00 | 0.00
Blue_cyan | 4796 | 1.46% | 158.79 | 175.00 | 164.36

```

Figure 38- Segment Information.

3.8.1.10. Export Temperature Matrix

The "*Export Temperature Matrix*" button is a function that allows exportation of the thermal data held in the image as a matrix, usually in a CSV (Comma-Separated Values) format file. This can be a very useful feature for further quantitative analysis, since it will take the temperature values of each pixel of the image and place them in a numeric matrix, where each element is the temperature expressed in degrees Celsius.

The output file is ready to be imported into other data processing programs, including Excel, Python, or MATLAB, for further analysis, graphing, or integration with other systems. The export includes a header of pixel coordinates (X/Y), thereby enhancing the readability and real-world usefulness of the data in scientific or industrial applications.

3.8.1.11. Open

The "*Open*" button enables the user to import thermal images in several formats, such as BMP, PNG, JPG, RAW, and IS2, among others. On selecting an image, the software performs initial processing operations, which include the conversion of the image into a temperature scale and noise reduction filtering, thereby making the image ready for analysis. The functionality outlined is fundamental in enabling the user to handle several thermal data sources independent of the initial image format. The Open button also serves to clear any previously conducted analyses, hence preparing the software to analyze a new image.

3.8.1.12. Save

The “*Save*” button provides the user with the option of saving processed images, including versions highlighting anomalies, directing attention to regions of interest, or mapping colors. The program allows images to be saved in formats like PNG, thereby maintaining the visual quality and nuances of the analyses performed. Besides, users can also store various versions of the same image, i.e., the original, the processed, and the one that detects anomalies, to easily document and share the findings. This functionality is required for report writing, presentation, or reference document creation that will be utilized for analysis in the future.

4. ANALYSIS OF THE RESULTS

To evaluate the effectiveness of the software developed for the automatic detection of building pathologies through thermal images, a series of practical tests was conducted using a set of pre-selected reference images. This chapter presents a systematic analysis of the results obtained from the application of the implemented functionalities, with a focus on verifying the system's capability to highlight thermal anomalies related to construction defects such as moisture infiltration, thermal bridges, and delamination.

The tests were performed using a database composed of 16 reference thermal images, previously used in academic research. Each image was sequentially processed through the main steps of the proposed workflow: noise removal, temperature calibration, application of colormaps, thermal segmentation, and anomaly detection using both percentile and color-based methods.

The analysis aims to assess the tool's performance under different image conditions and thermal complexities, identifying its strengths, limitations, and opportunities for improvement. Whenever possible, the results are illustrated through comparative images (before and after processing), accompanied by technical commentary highlighting the tool's visual effectiveness, as well as discussions of any challenges or limitations encountered during usage.

4.1. Pre-processing and noise removal

The presence of thermal noise in raw infrared images can significantly impair the accuracy of segmentation and anomaly detection processes. To address this, the software includes a pre-processing step that allows the application of three types of filters: median, Gaussian, and bilateral. Each filter is designed to reduce noise while preserving relevant thermal gradients, which are essential for the identification of construction pathologies.

In the reference image (Figure 39), used for testing, the median filter proved effective in removing salt-and-pepper noise without distorting temperature contours.

The Gaussian filter smoothed the image more aggressively, which was useful for eliminating small fluctuations but sometimes reduced edge sharpness. The bilateral filter, although computationally more intensive, offered a good compromise by preserving edge definition while reducing local noise.

Figure 40 presents the same image before any noise removal, clearly illustrating the presence of thermal artifacts.

After applying the median filter (Figure 41) demonstrates the resulting improvement in image clarity and reduction of interference.

After filtering, regions with subtle thermal differences became more distinguishable, enhancing the performance of subsequent tools such as temperature segmentation and anomaly detection.

The user can choose the most appropriate filter depending on the characteristics of the image. In general, for images with well-defined thermal patterns, the median filter was sufficient. For noisier images, the bilateral filter produced clearer results. The software maintains the original image for comparison and allows iterative application of filters to optimize clarity before calibration and segmentation.

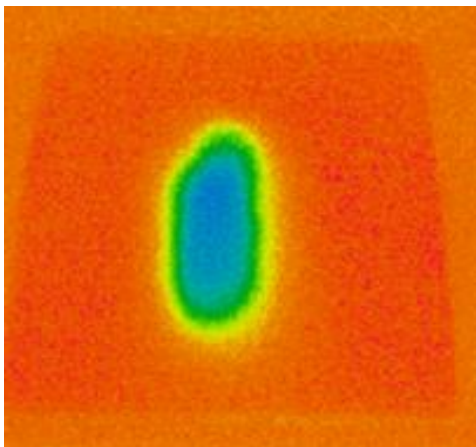


Figure 39- Reference image.

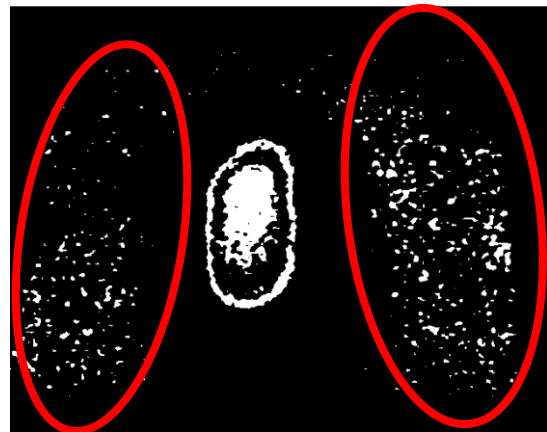


Figure 40- Image before remove noise.



Figure 41- Image after remove noise.

4.2. Temperature calibration

Thermal calibration is a critical step in ensuring that the temperature values represented in the image correspond accurately to real-world measurements. Without proper calibration, the software may interpret the thermal gradients incorrectly, leading to false positives or missed anomalies during the detection process.

In the software, calibration is performed by manually entering the minimum and maximum temperature values corresponding to the thermal image, as provided by the camera metadata or external measurement references. Once these values are entered, the temperature scale of the image is automatically adjusted, and a new colormap is generated to reflect the calibrated temperature range.

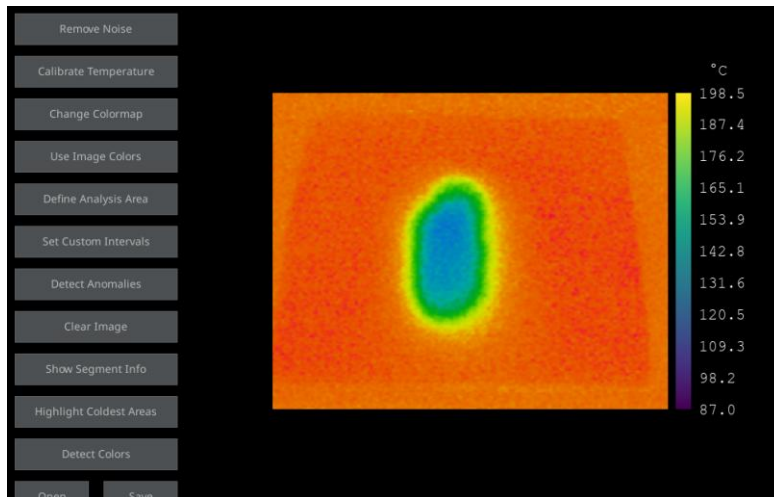
The process begins with the raw thermal image, shown in Figure 42 (a), which includes a default (non-calibrated) scale. In this state, the temperature distribution is visually represented, but the numerical values may not correspond to actual thermal conditions.

The calibration process ensures that all subsequent segmentation and anomaly detection operations are based on reliable thermal information (Figure 42 (c)).

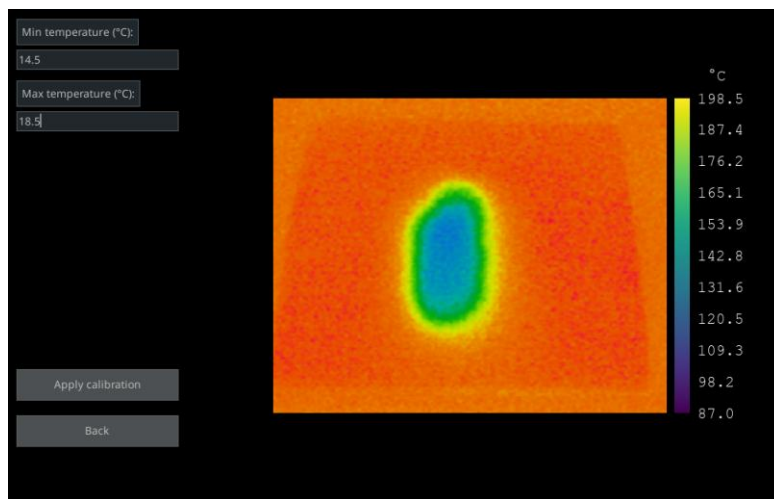
After calibration, the image is rescaled based on the new thermal limits, as illustrated in Figure 42 (b). The temperature bar is updated, and hovering the mouse over the image reveals the exact temperature of each pixel, enhancing the precision of the analysis.

This calibration is essential for interpreting the thermal data reliably, particularly when comparing multiple images or evaluating temperature thresholds in the detection of anomalies. Incorrect or absent calibration can result in misinterpretation of thermal patterns, especially when the original image is captured under varying environmental conditions.

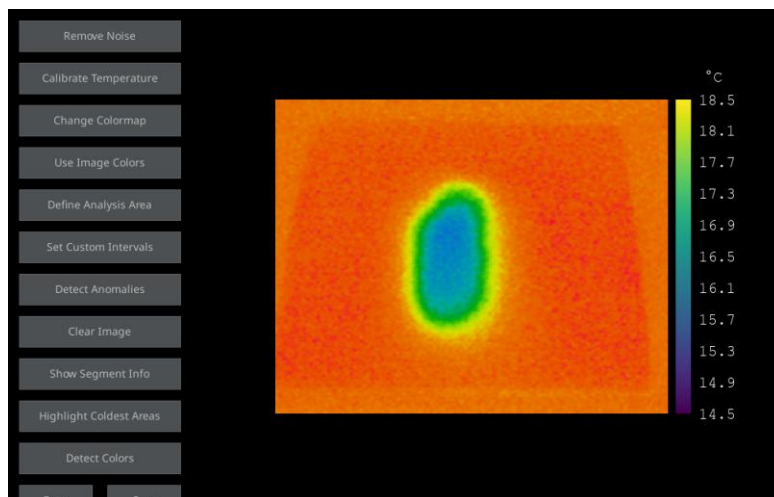
Therefore, it is recommended that the calibration be performed before applying segmentation or anomaly detection tools, ensuring that all subsequent analysis is based on accurate and consistent thermal data.



(a) Upload image with initial scale



(b) Applying temperatures in the calibrate temperature function



(c) New scale with determined minimum and maximum temperatures

Figure 42- Calibrate temperature

4.3. Change ColorMap

The ability to adjust the colormap is a key feature for improving the visual interpretation of thermal data. In raw or grayscale thermal images, subtle variations in temperature can be difficult to distinguish, especially when analyzing potential pathologies such as moisture accumulation or thermal bridging.

The software offers the option to apply several colormaps, including *Inferno*, *Viridis*, *Plasma*, and others. These color scales assign visual intensity to temperature values, enhancing contrast and facilitating the identification of anomalies.

Figure 43 shows a thermal image in its original grayscale representation. Although the overall thermal distribution is visible, low-contrast areas may make it difficult to identify subtle temperature anomalies.

After applying a color-based colormap, as shown in Figure 44, temperature differences become more evident. The use of high-contrast color gradients improves the readability of thermal zones and supports more accurate segmentation and anomaly detection.

Among the available options, colormaps like *Inferno* or *Plasma* were especially effective in emphasizing cold regions often associated with moisture or insulation failure. Conversely, *Viridis* and *Coolwarm* provided smoother gradients that are better suited for comparative analysis across different images.

The choice of colormap should be based on the objective of the inspection and the nature of the thermal patterns. By allowing flexible visualization, the software enhances the user's ability to detect and interpret structural anomalies with greater confidence.

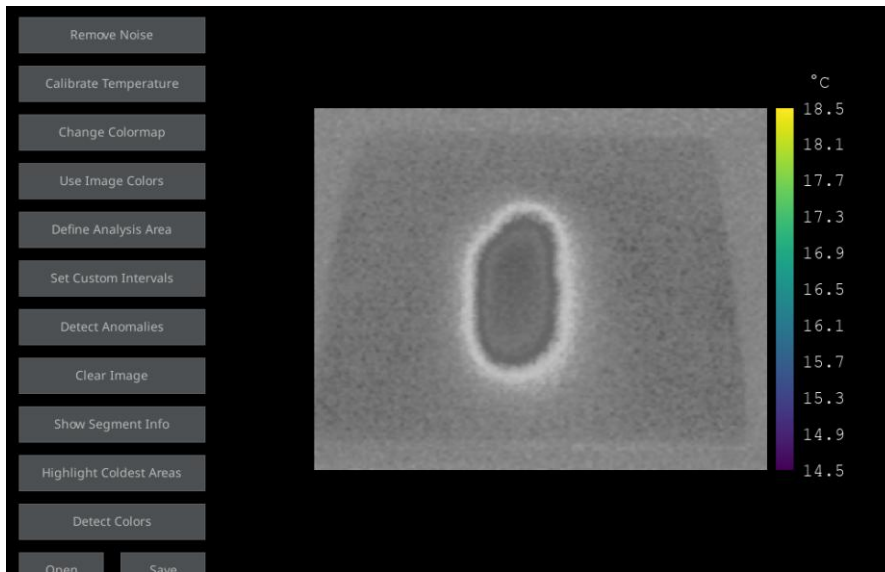


Figure 43- Black and white image.

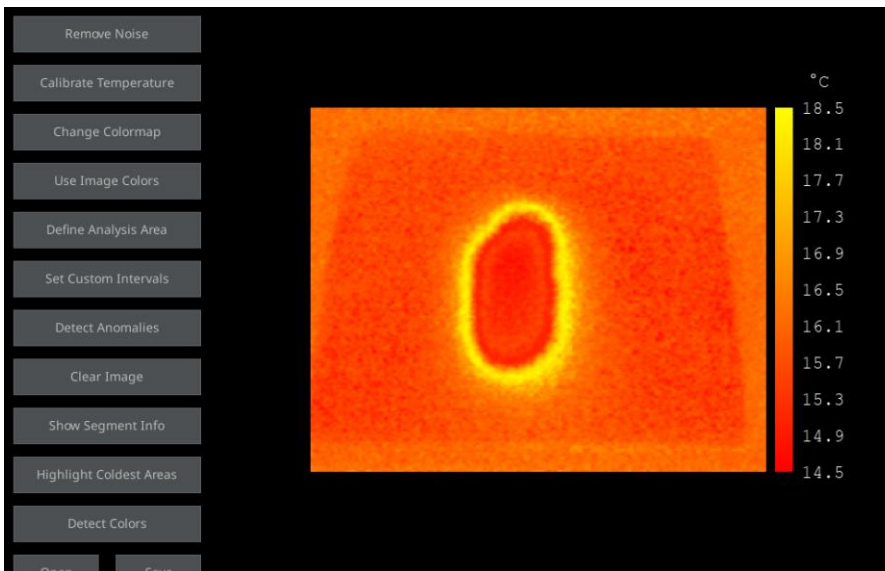


Figure 44- Coloured image.

4.4. Using Image Colors

The “*Use Image Colors*” function enables the user to visualize the thermal image exactly as it was originally recorded by the infrared camera, using its embedded native color scale. This approach can be useful in cases where the image was captured with a pre-configured thermal palette aligned with the camera’s internal calibration.

By preserving the original color coding, this function supports visual validation during field inspections or comparison with manufacturer-provided scales. It is particularly useful when interpreting images from devices with standardized colormaps or when correlating visual features with physical site observations.

However, the limited contrast of some native palettes may reduce the visibility of subtle temperature variations. In such cases, switching to enhanced colormaps (as discussed in Section 4.3) can help improve diagnostic clarity.

Figure 45 illustrates the result of applying the “*Use Image Colors*” function to a reference image. The thermal palette applied by the camera is retained, maintaining the original context of the data acquisition.

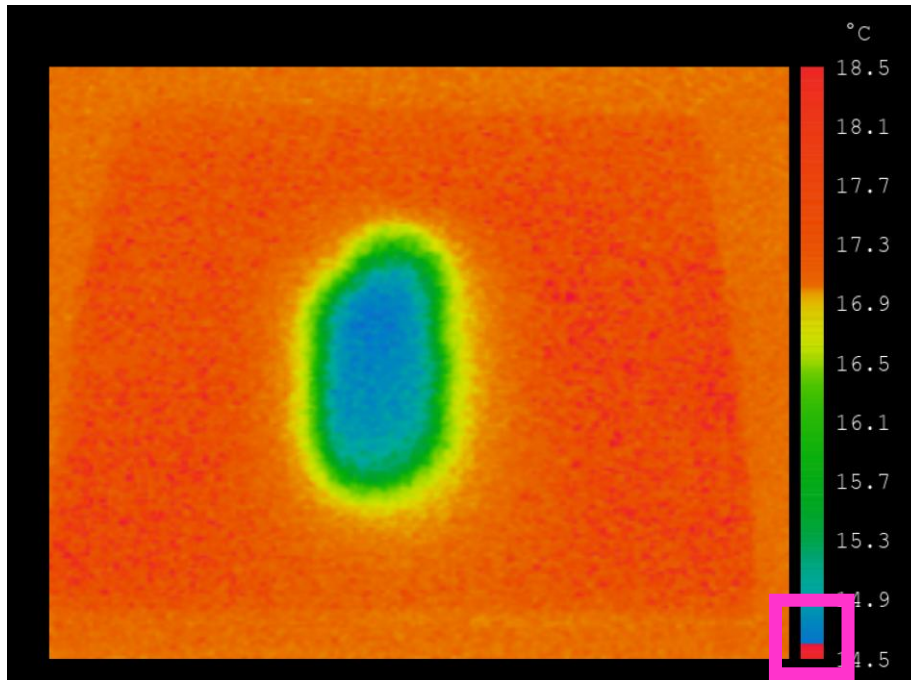
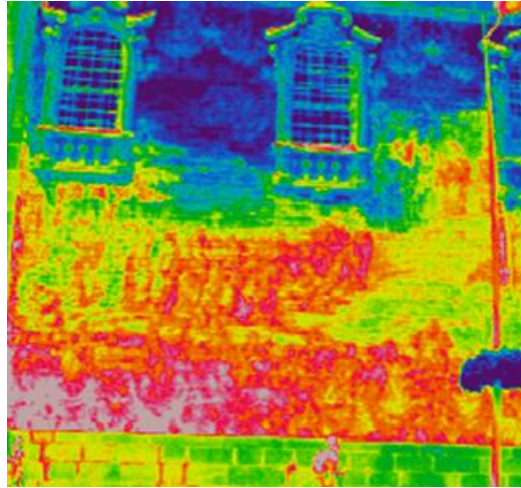


Figure 45- Image after using image colors.

4.5. Define analysis area

The defined analysis area function performs effectively when applied to images containing extensive anomaly regions or when the user intends to analyze only a specific section of the image, including the anomaly itself. This tool accurately isolates the selected area, enhancing its visualization and facilitating a more focused analysis.



As illustrated in Figure 46, the image contains a surface with multiple elements, making it challenging for the user to analyze it comprehensively. In cases where the objective is to examine a specific section, such as the windows, the define analysis area function proves particularly useful. By enabling the isolation of the desired region, it allows for a more precise assessment of the anomalies present, as demonstrated in Figure 47.

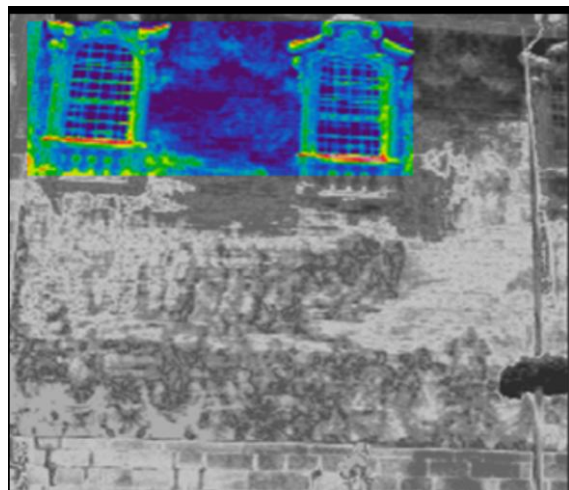
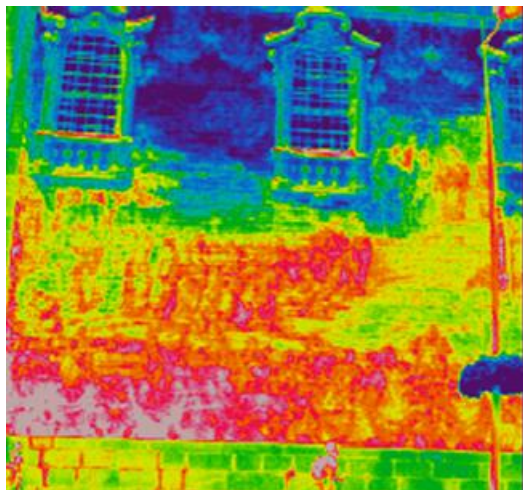


Figure 46- Image that contains many anomalies. Figure 47- Only the selected portion of the window.

4.6. Set customs intervals

The “*Set Custom Intervals*” function allows users to define specific temperature ranges for segmenting thermal images. This feature is especially valuable in scenarios where known thresholds are associated with particular pathologies—for example, identifying areas between 17.0 °C and 18.5 °C that may indicate moisture accumulation or heat loss. After defining one or more intervals, the software applies a binary segmentation mask, visually highlighting the pixels that fall within the selected range. This enables precise targeting of thermal zones for further inspection or documentation.

As shown in Figure 48, the result segmentation on the thermal image. Colored masks are applied to visually differentiate the selected ranges from the rest of the image, facilitating the identification of affected regions.

Figure 49 displays the user-defined temperature interval applied in this example, while This method offers a high degree of control and technical specificity. It is particularly effective when used in conjunction with field data or when analyzing materials with known thermal behavior.

Although it requires manual input from the user, it allows for precise targeting of thermal anomalies within defined temperature thresholds. For best results, it is recommended that the thermal image be properly calibrated prior to using this feature, ensuring that the selected values accurately reflect real-world temperatures.

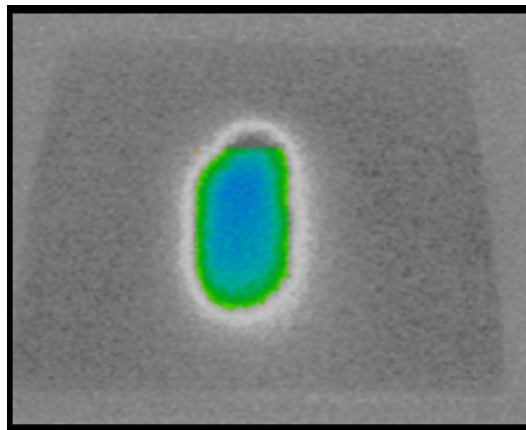


Figure 48- Image after the set custom intervals.

Data range: 14.5 to 17.4

Start:

End:

Step:

Figure 49- Defined interval.

4.7. Detect anomalies

The “*Detect Anomalies*” function applies a statistical thresholding technique based on user-defined percentiles to automatically highlight the coldest regions of the thermal image. This method is particularly useful for identifying potential pathologies such as

moisture infiltration or thermal bridges, which typically manifest as localized low-temperature zones.

The algorithm calculates the selected percentile (e.g., the 5th percentile) and creates a binary mask that isolates the pixels below this value. These areas are then highlighted visually, allowing for immediate recognition of anomalous regions without the need for predefined temperature ranges.

Figure 50 presents a visual comparison of this process. Subfigure (a) shows the original thermal image before any processing, while subfigure (b) illustrates the result of applying the “*Detect Anomalies*” function with a 5% threshold. The coldest regions are masked in white, drawing attention to potentially critical areas that merit further inspection.

This approach is advantageous in that it requires minimal user input and adapts dynamically to each image’s thermal distribution. However, it may produce false positives in images with shadows, emissivity inconsistencies, or non-uniform surfaces. In such cases, visual validation or cross-checking with field data is recommended to confirm the presence of actual anomalies.

Overall, percentile-based anomaly detection offers a fast and accessible solution for identifying areas of interest, especially in large datasets or initial screening processes.



Figure 50- Visual comparison illustrating anomaly detection: (a) original thermal image and (b) image processed with the detect anomalies function.

4.8. Detect colors

The “*Detect Colors*” function enables the user to isolate specific regions of a thermal image based on color similarity. This approach is particularly useful when working with

images that are not thermally calibrated, but in which color gradients follow a recognizable pattern — for instance, dark blue for cold zones or bright red for hot areas. Using a color picker interface, the user selects a target color within the image. The software then identifies all pixels within a defined RGB tolerance range and generates a mask highlighting the detected area. This tool allows for intuitive analysis, especially for users less familiar with temperature scales or statistical thresholds.

Figure 51 provides a side-by-side comparison of this process. Subfigure (a) presents the original thermal image, while subfigure (b) displays the result after applying the “Detect Colors” function. The selected color — associated with colder areas — has been effectively isolated, supporting the visual identification of potentially problematic zones.

Although this method is highly accessible and visually immediate, it has some limitations. Its accuracy depends on the consistency of the color mapping and is sensitive to factors such as image compression, lighting variation, and display artifacts. Therefore, color-based detection is best used as a complementary tool, especially when calibration data is unavailable or when quick visual segmentation is needed.

In practical terms, this function enhances usability for preliminary assessments and educational contexts, and it serves as an entry-level method for identifying thermal anomalies without requiring technical expertise in temperature analysis.



Figure 51- Visual comparison illustrating anomaly detection: (a) original thermal image and (b) image processed with the detect colors function.

4.9. Show segment info

To validate the functionality of the show segment info feature, the reference image shown in Figure 52 was used for sampling. A specific analysis area (Figure 53) and a temperature

range (Figure 54) were defined. The range was segmented according to a user-established interval, which in this case was set to 1 °C. The resulting data are presented in Table 3, Table 4, Table 5. It is evident that the results are conclusive, and, unlike other functions, they provide information in a measurable form, which is essential for detailed and precise analysis by the user.

The capacity of the show segment info tool to deliver quantifiable and statistical details plays a vital role in undertaking an objective and complete analysis. By giving numerical values like area in pixels, representative percentage, mean temperature, and standard deviation, the tool not only allows users to view, but also comprehends the nature of the area being studied in exact, quantifiable form. This enables more effective evaluation of the thermal distribution in the image. The color-based analysis provides data such as areas, representative percentage, minimum temperature, maximum temperature, and standard deviation, allowing for the user an even more detailed understanding of thermal variations.

For the image chosen, the results obtained were as follows: minimum temperature of 14.5 °C, maximum temperature of 17.37 °C, mean temperature of 16.1 °C, median temperature of 16.20 °C, and standard deviation of 0.64 °C. These statistical measures are important as they allow for the quantitative examination of thermal variations, thereby enhancing the precision and validity of the interpretation of the results, which enables decision-making to be more informed, and evidence based.

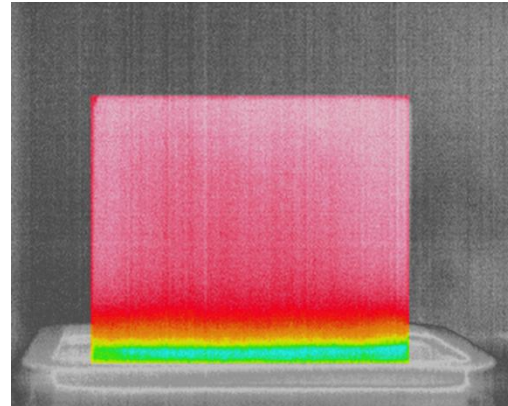
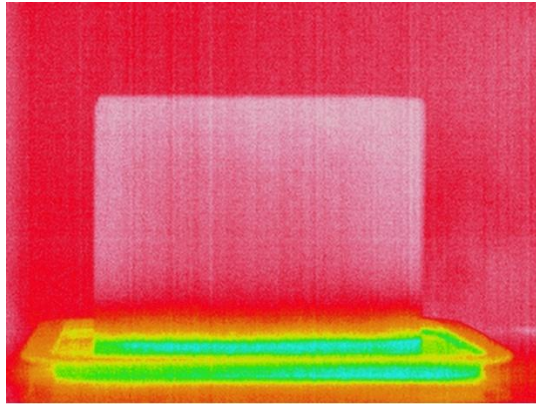


Figure 52- Reference image for the show segment info. Figure 53- Image of the area selected for analysis.

Data range: 14.5 to 17.4

Start:

End:

Step:

Figure 54- Range of temperatures to choose.

Temperature Segment Information				
Temperature Range	Area (px)	% Total	Avg Temp (°C)	Std Dev (°C)
14.5°C - 15.5°C	23448	17.74%	15.02	0.29
15.5°C - 16.5°C	68847	52.08%	16.07	0.27
16.5°C - 17.5°C	39906	30.19%	16.79	0.19

Table 3- Result of segment information.

Information of Color-Detected Areas					
Color	Area (px)	% Total	Min Temp (°C)	Max Temp (°C)	Avg Temp (°C)
Blue	0	0.00%	0.00	0.00	0.00
Green	2675	2.02%	16.12	16.35	16.19
Cyan	2835	2.14%	16.36	16.72	16.48
Yellow	4713	3.57%	16.34	17.17	16.84
Purple	0	0.00%	0.00	0.00	0.00
Blue Cyan	2835	2.14%	16.36	16.72	16.48

Table 4- Information of color detect areas.

Analysis Area Statistics
Min: 14.50°C
Max: 17.37°C
Mean: 16.11°C
Median: 16.20°C
Std: 0.64°C

Table 5- Statistical data of the analysed area.

4.10. Clear image

The clear image button resets both the area definition functions, and the range previously set by the user. This functionality operates effectively, enabling the user to analyze different regions of the image without the need to reopen it.

4.11. Export matrix

The export matrix function enables the program to generate a CSV file containing the coordinates and corresponding data for each pixel in the image. This allows the user to study the temperature data in more detail using independent software such as MATLAB or Excel. The data exported can also be utilized for long-term studies since the data is stored for future reference. Although the program effectively exports the data, temperatures in this file were not compared within the framework of this study.

5. CONCLUSION AND FUTURE WORKS

This research aimed to develop and evaluate a software tool for the automatic detection of anomalies in buildings based on thermal images, with emphasis on accessibility, lightweight implementation, and technical applicability in construction diagnostics.

The software integrates several processing functionalities, including noise removal filters, temperature calibration, colormap customization, and segmentation tools based on both statistical thresholds and visual cues. These features enable users to analyze thermal patterns and highlight potential pathologies such as moisture infiltration or insulation failure.

Among the implemented methods, the percentile-based anomaly detection proved to be efficient in highlighting the coldest regions of the image automatically, while the custom interval segmentation allowed for more precise control when specific temperature ranges were known. The use of color-based detection added an intuitive option for non-calibrated images, especially useful in practical scenarios.

The results demonstrate that the tool can assist in the preliminary diagnosis of thermal anomalies in buildings, offering an affordable and portable alternative to more complex systems. Its graphical interface and modular design make it suitable for technicians, engineers, or researchers working in building inspection and preventive maintenance.

However, the study presents some limitations. The small dataset of thermal images prevented the use of machine learning models and limited the statistical validation of the results. Additionally, the lack of field-based comparisons such as physical inspection data, constrained the empirical evaluation of the tool's accuracy. Finally, the absence of real-time sensor integration means the system currently depends on pre-captured static images.

In summary, the developed software fulfills its intended purpose and demonstrates technical viability. It offers a practical contribution to the field of building diagnostics, especially in low-resource contexts, and lays the groundwork for future technological advancements in automated thermal analysis.

For future work, the following improvements are proposed:

- Expansion of the image dataset to support machine learning approaches, such as convolutional neural networks;

- Integration with real-time thermal sensors, allowing dynamic data acquisition;
- Validation of the tool through on-site experiments and comparison with traditional inspection methods;
- Enhancement of the anomaly classification system, potentially distinguishing between different types of pathologies.

REFERENCES

- [1] S. Bagavathiappan, B. B. Lahiri, T. Saravanan, J. Philip, e T. Jayakumar, “Infrared thermography for condition monitoring - A review”, 2013. doi: 10.1016/j.infrared.2013.03.006.
- [2] N. P. Avdelidis e A. Moropoulou, “Applications of infrared thermography for the investigation of historic structures”, 2004, *Elsevier Masson SAS*. doi: 10.1016/j.culher.2003.07.002.
- [3] E. Barreira e V. P. de Freitas, “Evaluation of building materials using infrared thermography”, *Constr Build Mater*, vol. 21, no 1, p. 218–224, jan. 2007, doi: 10.1016/j.conbuildmat.2005.06.049.
- [4] R. Usamentiaga, P. Venegas, J. Guerediaga, L. Vega, J. Molleda, e F. G. Bulnes, “Infrared thermography for temperature measurement and non-destructive testing”, 10 de julho de 2014, *MDPI AG*. doi: 10.3390/s140712305.
- [5] A. Wilson, K. Gupta, B. H. Koduru, A. Kumar, A. Jha, e L. R. Cenkeramaddi, “Recent Advances in Thermal Imaging and its Applications Using Machine Learning: A Review”, *IEEE Sens J*, vol. PP, p. 1, fev. 2023, doi: 10.1109/JSEN.2023.3234335.
- [6] *fib Bulletin 65 - Model Code for Concrete Structures 2010*. International Federation for Structural Concrete (fib), 2012.
- [7] “EN 1992-1-1: Eurocode 2: Design of concrete structures - Part 1-1: General rules and rules for buildings”, 2004.
- [8] “ACI 365.1R-00. Service-Life Prediction-State-of-the-Art Report”, 2000.
- [9] “UN Sustainable Development Goals (2023). Goal 11: Sustainable Cities and Communities.”, 2023. [Online]. Disponível em: <https://www.globalgoals.org/goals/11-sustainable-cities-and-communities/>
- [10] J. Jorge Almeida Rodrigues, “Proteção e Reabilitação de Estruturas de Betão Armado”, 2017.
- [11] “EN 1992-1-1: Eurocode 2: Design of concrete structures - Part 1-1: General rules and rules for buildings”, 2004.

- [12] Isabela Soraia Costa Gomes, “Deterioração do betão: Técnicas de Avaliação e Prevenção”, 2016.
- [13] J. A. L. M. Padrão, “Técnicas de Inspeção e Diagnóstico em Estruturas”, 2004.
- [14] E. Edis, I. Flores-Colen, e J. De Brito, “Time-Dependent Passive Building Thermography for Detecting Delamination of Adhered Ceramic Cladding”, *J Nondestr Eval*, vol. 34, no 3, fev. 2015, doi: 10.1007/S10921-015-0297-5.
- [15] I. Garrido, S. Lagüela, S. Sfarra, F. J. Madruga, e P. Arias, “Automatic detection of moistures in different construction materials from thermographic images”, *J Therm Anal Calorim*, vol. 138, no 2, p. 1649–1668, fev. 2019, doi: 10.1007/S10973-019-08264-Y.
- [16] W. liang Qiu, R. xin Peng, e M. Jiang, “Meso equivalent calculation model for frost evaluation of concrete”, *Constr Build Mater*, vol. 272, fev. 2021, doi: 10.1016/j.conbuildmat.2020.121867.
- [17] R. Xin Peng, W. Liang Qiu, e F. Teng, “Three-dimensional meso-numerical simulation of heterogeneous concrete under freeze-thaw”, *Constr Build Mater*, vol. 250, jul. 2020, doi: 10.1016/j.conbuildmat.2020.118573.
- [18] V. Custódio, M. De Souza, e T. Ripper, “PATOLOGIA E REFORÇO DE CONCRETO”.
- [19] T. Aberle, E. Switzerland, A. Keller, e R. Zurbriggen, “Efflorescence Mechanisms of Formation and Ways to Prevent”.
- [20] C. Dow e F. P. Glasser, “Calcium carbonate efflorescence on Portland cement and building materials”, *Cem Concr Res*, vol. 33, no 1, p. 147–154, jan. 2003, doi: 10.1016/S0008-8846(02)00937-7.
- [21] B. Kanagaraj, R. Priyanka, N. Anand, T. Kiran, A. D. Andrushia, e E. Lubloy, “A sustainable solution for mitigating environmental corrosion in the construction sector and its socio-economic concern”, *Case Studies in Construction Materials*, vol. 20, jul. 2024, doi: 10.1016/j.cscm.2024.e03089.
- [22] A. Zomorodian e A. Behnood, “Review of Corrosion Inhibitors in Reinforced Concrete: Conventional and Green Materials”, 1o de maio de 2023, *MDPI*. doi: 10.3390/buildings13051170.

- [23] C. Jiang, L. Jiang, X. Tang, J. Gong, e H. Chu, “Impact of calcium leaching on mechanical and physical behaviors of high belite cement pastes”, *Constr Build Mater*, vol. 286, jun. 2021, doi: 10.1016/j.conbuildmat.2021.122983.
- [24] H. Al-Khayat, M. Haque, e N. Fattuhi, “Concrete carbonation in arid climate”, *Materials and Structures/Materiaux et Constructions*, vol. 35, p. 421–426, fev. 2002, doi: 10.1007/BF02483146.
- [25] B. Fournier e M. Bérubé, “Alkali-aggregate reaction in concrete: A review of basic concepts and engineering implications”, *Canadian Journal of Civil Engineering*, vol. 27, p. 167–191, fev. 2011, doi: 10.1139/cjce-27-2-167.
- [26] S. Wei, Z. Jiang, H. Liu, D. Zhou, e M. Sanchez-Silva, “Microbiologically induced deterioration of concrete-A Review”, 2013. [Online]. Disponível em: www.sbmicrobiologia.org.br
- [27] J. B. Luz, I. de O. Silveira, e M. A. R. Soeiro, “Ensaio termográfico de edificação histórica: Igreja de Nossa Senhora da Conceição de Almofala / Thermographic test of historical heritage: Igreja de Nossa Senhora da Conceição de Almofala”, *Brazilian Journal of Development*, vol. 7, no 10, p. 100708–100731, out. 2021, doi: 10.34117/bjdv7n10-401.
- [28] R. L. Burity Filho, Y. H. D. M. de Luna, M. R. F. Lima Filho, e G. B. Athayde Júnior, “Aplicação da termografia na identificação de infiltrações e tubulações para condução de água fria e água quente embutidas em alvenaria”, *Research, Society and Development*, vol. 10, no 8, p. e34610817480, jul. 2021, doi: 10.33448/rsd-v10i8.17480.
- [29] L. A. de P. Junior e M. de J. R. da Nóbrega, “Detecção de infiltrações por meio de ensaios não destrutivos: um estudo de caso”, *Brazilian Journal of Development*, vol. 8, no 12, p. 80052–80071, dez. 2022, doi: 10.34117/bjdv8n12-216.
- [30] I. Garrido, E. Barreira, R. M.S.F. Almeida, e S. Lagüela, “Introduction of active thermography and automatic defect segmentation in the thermographic inspection of specimens of ceramic tiling for building façades”, *Infrared Phys Technol*, vol. 121, mar. 2022, doi: 10.1016/j.infrared.2021.104012.

- [31] I. Garrido, S. Lagüela, R. Otero, e P. Arias, “Thermographic methodologies used in infrastructure inspection: A review—Post-processing procedures”, 15 de maio de 2020, *Elsevier Ltd.* doi: 10.1016/j.apenergy.2020.114857.
- [32] A. François, L. Ibos, V. Feuillet, e J. Meulemans, “In situ measurement method for the quantification of the thermal transmittance of a non-homogeneous wall or a thermal bridge using an inverse technique and active infrared thermography”, *Energy Build*, vol. 233, fev. 2021, doi: 10.1016/j.enbuild.2020.110633.
- [33] B. Bielek, D. Szabó, J. Čurpek, P. Suchánek, e P. Panáček, “Infrared Thermography Diagnostics of Air Permeability Through Building Openings – Assessment of its Reliability”, *Slovak Journal of Civil Engineering*, vol. 28, no 1, p. 25–32, mar. 2020, doi: 10.2478/sjce-2020-0004.
- [34] E. Bauer, P. M. Milhomem, e L. A. G. Aidar, “Evaluating the damage degree of cracking in facades using infrared thermography”, *J Civ Struct Health Monit*, vol. 8, no 3, p. 517–528, jul. 2018, doi: 10.1007/s13349-018-0289-0.
- [35] I. Garrido, S. Lagüela, R. Otero, e P. Arias, “Thermographic methodologies used in infrastructure inspection: A review—data acquisition procedures”, 1o de dezembro de 2020, *Elsevier B.V.* doi: 10.1016/j.infrared.2020.103481.
- [36] N. Živanović, M. Aškračić, A. Savić, M. Stević, e Z. Stević, “Early-Age Cement Paste Temperature Development Monitoring Using Infrared Thermography and Thermo-Sensors”, *Buildings*, vol. 13, no 5, maio 2023, doi: 10.3390/buildings13051323.
- [37] N. P. Avdelidis e A. Moropoulou, “Applications of infrared thermography for the investigation of historic structures”, *J Cult Herit*, vol. 5, no 1, p. 119–127, jan. 2004, doi: 10.1016/J.CULHER.2003.07.002.
- [38] I. Garrido, S. Lagüela, S. Sfarra, F. J. Madruga, e P. Arias, “Automatic detection of moistures in different construction materials from thermographic images”, *J Therm Anal Calorim*, vol. 138, no 2, p. 1649–1668, out. 2019, doi: 10.1007/S10973-019-08264-Y.
- [39] R. Usamentiaga, P. Venegas, J. Guerediaga, L. Vega, J. Molleda, e F. G. Bulnes, “Infrared thermography for temperature measurement and non-destructive testing”, 10 de julho de 2014, *MDPI AG.* doi: 10.3390/s140712305.

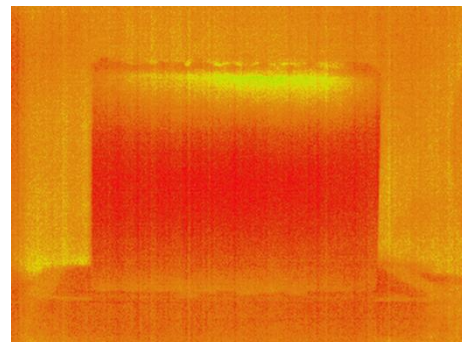
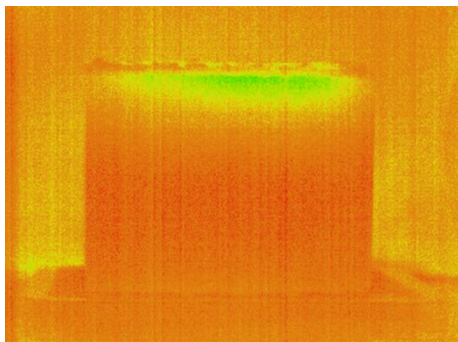
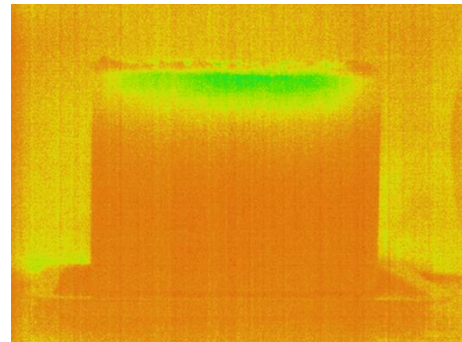
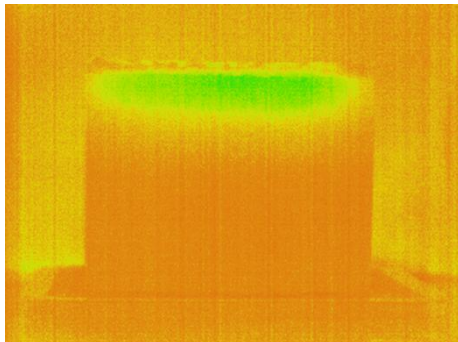
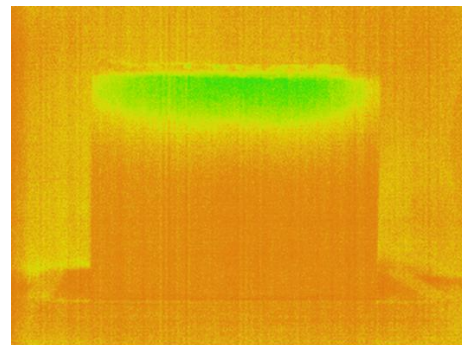
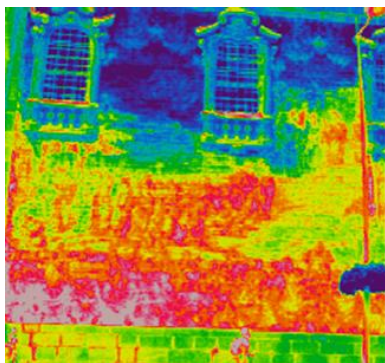
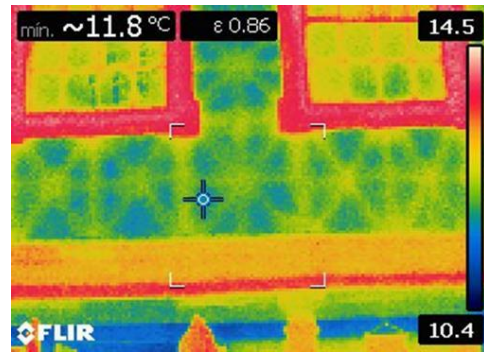
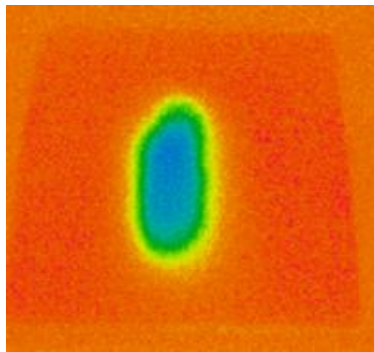
- [40] A. François, L. Ibos, V. Feuillet, e J. Meulemans, “In situ measurement method for the quantification of the thermal transmittance of a non-homogeneous wall or a thermal bridge using an inverse technique and active infrared thermography”, *Energy Build*, vol. 233, p. 110633, fev. 2021, doi: 10.1016/J.ENBUILD.2020.110633.
- [41] Q. Fang, C. Ibarra-Castanedo, I. Garrido, Y. Duan, e X. Maldague, “Automatic Detection and Identification of Defects by Deep Learning Algorithms from Pulsed Thermography Data”, *Sensors*, vol. 23, no 9, maio 2023, doi: 10.3390/s23094444.
- [42] Y. He *et al.*, “Infrared machine vision and infrared thermography with deep learning: A review”, 1o de agosto de 2021, *Elsevier B.V.* doi: 10.1016/j.infrared.2021.103754.
- [43] C. Kim, J. S. Choi, H. Jang, e E. J. Kim, “Automatic detection of linear thermal bridges from infrared thermal images using neural network”, *Applied Sciences (Switzerland)*, vol. 11, no 3, p. 1–14, fev. 2021, doi: 10.3390/app11030931.
- [44] M. Gil-Docampo, J. O. Sanz, I. C. Guerrero, e M. F. Cabanas, “UAS IR-Thermograms Processing and Photogrammetry of Thermal Images for the Inspection of Building Envelopes”, *Applied Sciences (Switzerland)*, vol. 13, no 6, mar. 2023, doi: 10.3390/app13063948.
- [45] M. Anuar, N. Sarbini, I. Ibrahim, S. Othman, e M. Reba, “Building condition ratings using infrared thermography: a preliminary study”, *Archives of Civil Engineering*, p. 403–418, fev. 2022, doi: 10.24425/ace.2022.143046.
- [46] Y. Yao, S. Sfarra, C. Ibarra-Castanedo, R. You, e X. P. V Maldague, “The multi-dimensional ensemble empirical mode decomposition (MEEMD)”, *J Therm Anal Calorim*, vol. 128, no 3, p. 1841–1858, 2017, doi: 10.1007/s10973-016-6082-6.
- [47] B. C. F. de Oliveira, H. B. Fröhlich, E. S. Barrera, C. R. Baldo, A. A. G. Jr., e R. Schmitt, “Impact damage characterization in CFRP plates using PCA and MEEMD decomposition methods in optical lock-in thermography phase images”, em *Optical Measurement Systems for Industrial Inspection XI*, P. Lehmann, W. Osten, e A. A. G. Jr., Orgs., SPIE, 2019, p. 110562N. doi: 10.1117/12.2526357.

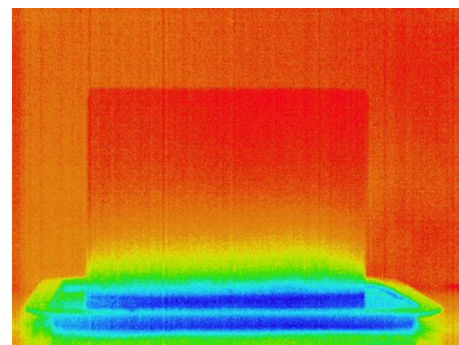
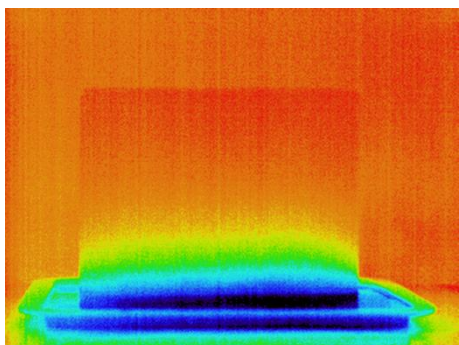
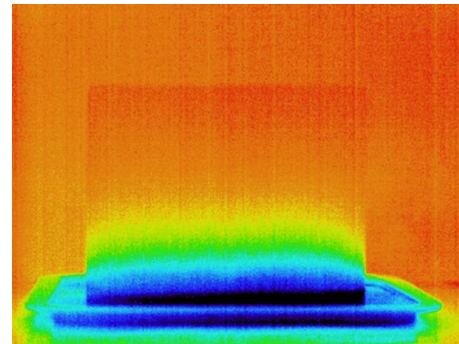
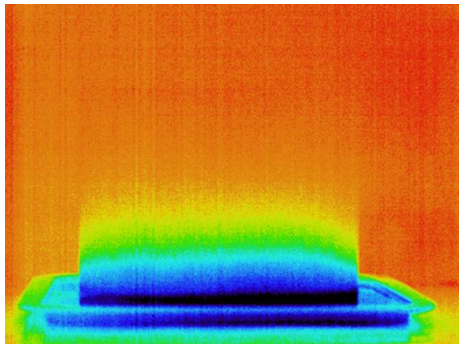
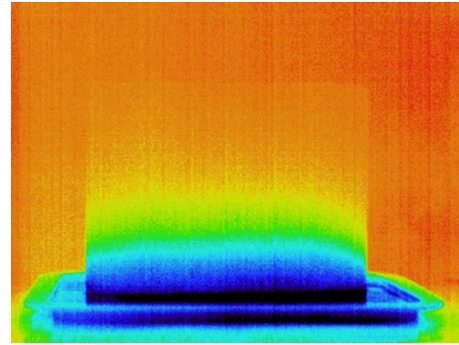
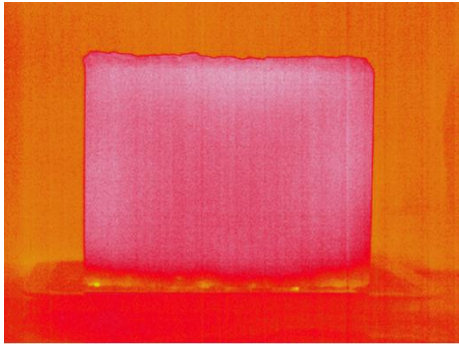
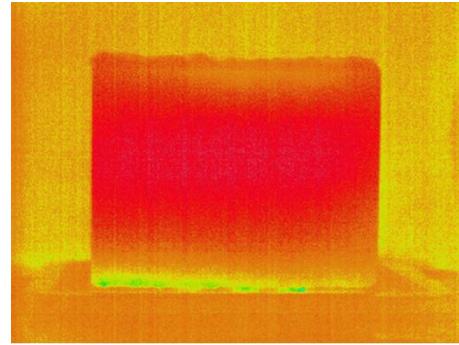
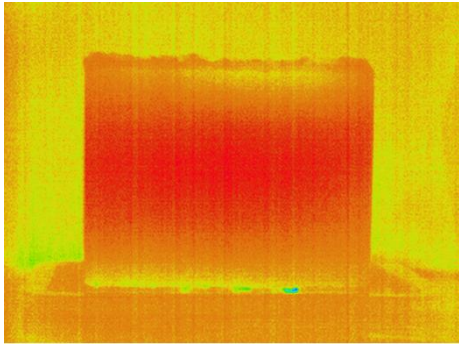
- [48] K. Tu, C. Ibarra-Castanedo, S. Sfarra, Y. Yao, e X. P. V. Maldague, “Multiscale analysis of solar loading thermographic signals for wall structure inspection†”, *Sensors*, vol. 21, no 8, abr. 2021, doi: 10.3390/s21082806.
- [49] Y. Sharrab *et al.*, “Performance Comparison of Several Deep Learning-Based Object Detection Algorithms Utilizing Thermal Images”, fev. 2021, p. 16–22. doi: 10.1109/IDSTA53674.2021.9660820.
- [50] D. Moher *et al.*, “Preferred reporting items for systematic reviews and meta-analyses: The PRISMA statement”, 1o de julho de 2009, *Public Library of Science*. doi: 10.1371/journal.pmed.1000097.
- [51] O. Zawacki-Richter, M. Kerres, S. Bedenlier, M. Bond, e K. Buntins Eds, “Systematic Reviews in Educational Research”.
- [52] N. van Eck e L. Waltman, “VOSviewer - Visualizing scientific landscapes”. [Online]. Disponível em: <https://www.vosviewer.com/>
- [53] A. S. F. C. e Almeida, A. J. A. Ornelas, e A. R. Cordeiro, “Termografia passiva no diagnóstico de patologias e desempenho térmico em fachadas de edifícios através de câmara térmica instalada em drone. Abordagem preliminar em Coimbra (Portugal)”, *Cadernos de Geografia*, no 42, p. 27–41, dez. 2020, doi: 10.14195/0871-1623_42_2.
- [54] V. Chidurala e X. Li, “Occupancy Estimation Using Thermal Imaging Sensors and Machine Learning Algorithms”, *IEEE Sens J*, vol. 21, no 6, p. 8627–8638, mar. 2021, doi: 10.1109/JSEN.2021.3049311.
- [55] L. C. M. Dafico, E. Barreira, R. M. S. F. Almeida, e R. Vicente, “Machine learning models applied to moisture assessment in building materials”, *Constr Build Mater*, vol. 405, nov. 2023, doi: 10.1016/j.conbuildmat.2023.133330.
- [56] Z. Li, Y. Jin, X. Liang, e J. Zeng, “Thermography evaluation of defect characteristics of building envelopes in urban villages in Guangzhou, China”, *Case Studies in Construction Materials*, vol. 17, dez. 2022, doi: 10.1016/j.cscm.2022.e01373.
- [57] M. Mahmoodzadeh, V. Gretka, S. Wong, T. Froese, e P. Mukhopadhyaya, “Evaluating patterns of building envelope air leakage with infrared thermography”, *Energies (Basel)*, vol. 13, no 14, jul. 2020, doi: 10.3390/en13143545.

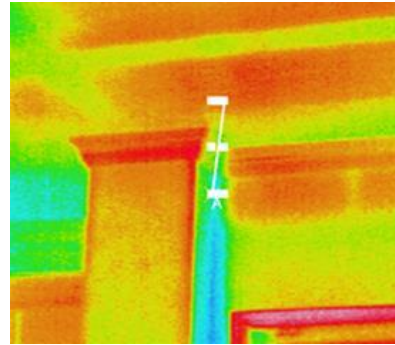
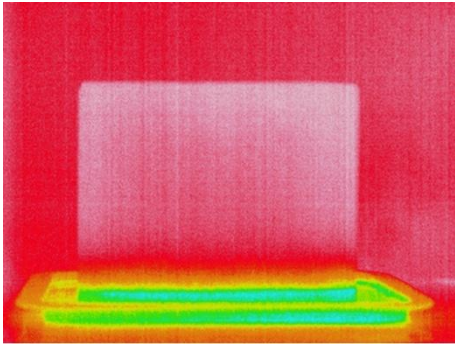
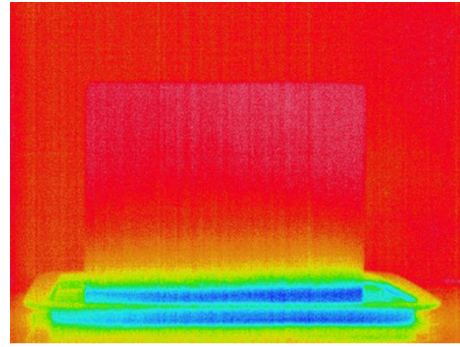
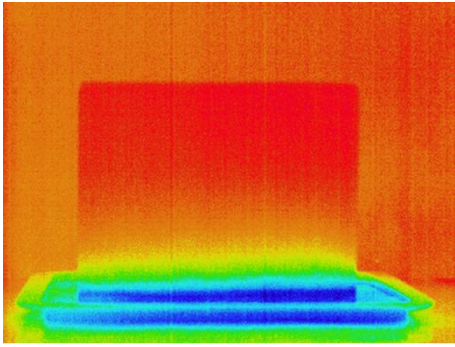
- [58] D. Sadhukhan *et al.*, “Estimating surface temperature from thermal imagery of buildings for accurate thermal transmittance (U-value): A machine learning perspective”, *Journal of Building Engineering*, vol. 32, nov. 2020, doi: 10.1016/j.jobbe.2020.101637.
- [59] E. Barreira, R. M. S. F. Almeida, e J. P. B. Ferreira, “Assessing the humidification process of lightweight concrete specimens through infrared thermography”, em *Energy Procedia*, Elsevier Ltd, 2017, p. 213–218. doi: 10.1016/j.egypro.2017.09.757.

6. ANNEX

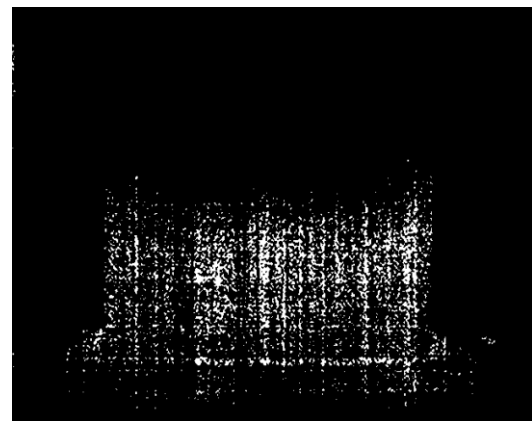
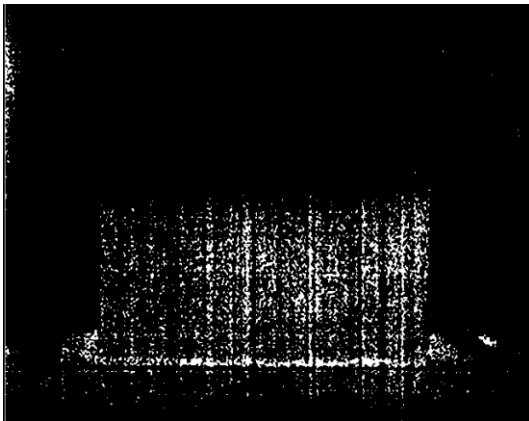
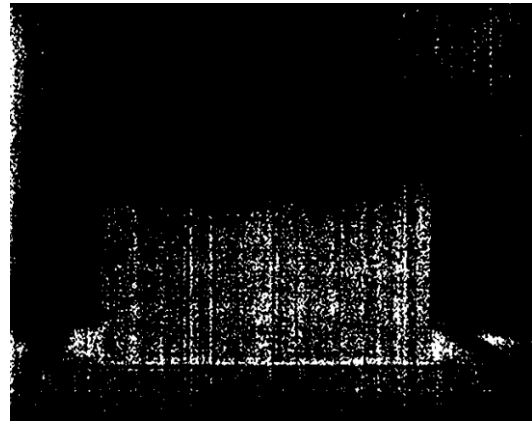
6.1. ANNEX A – Imagens de referência utilizadas no programa

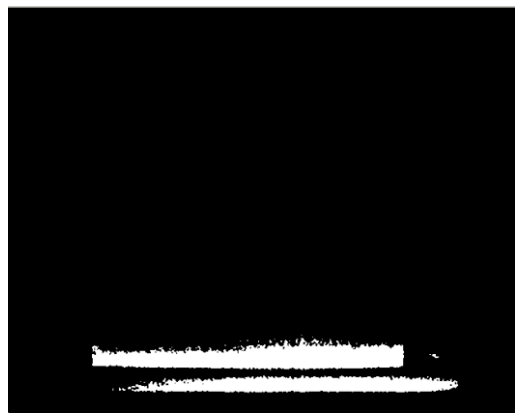
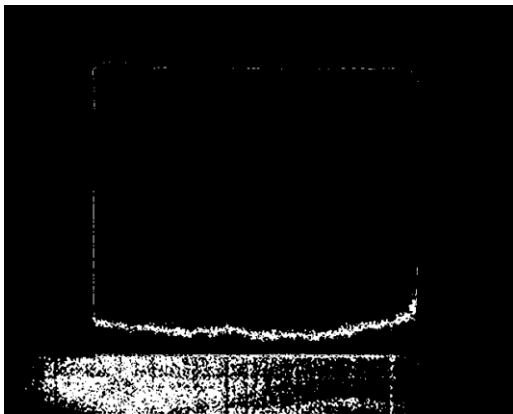
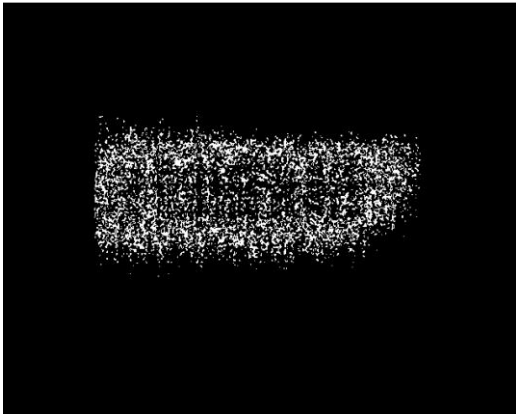
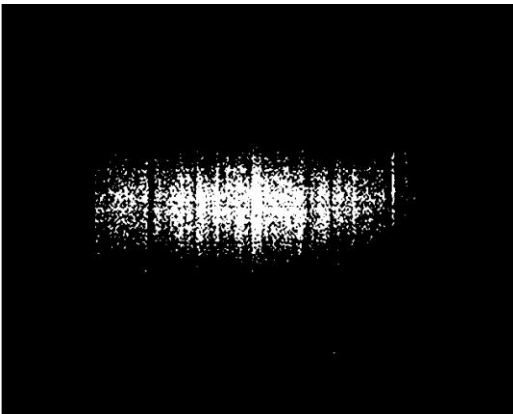
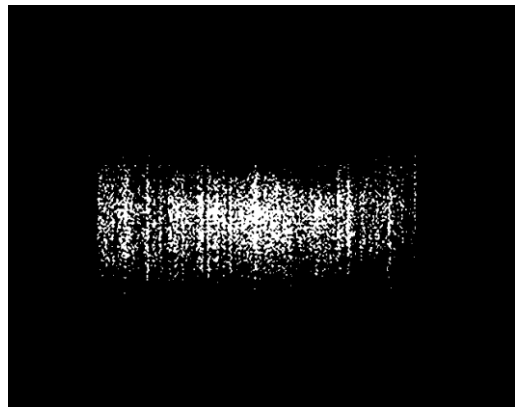
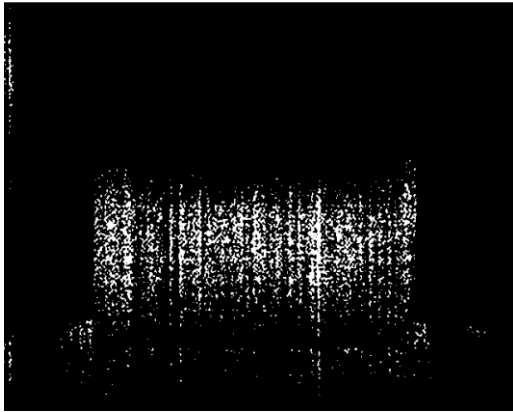


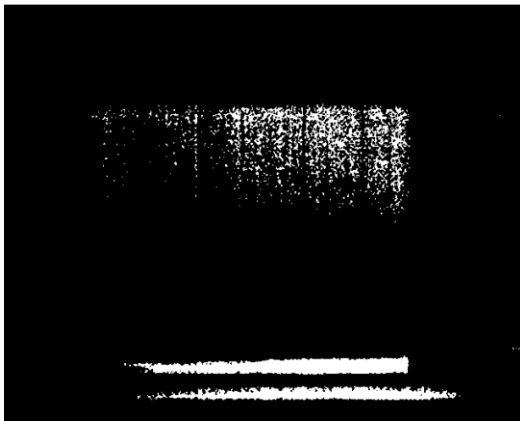
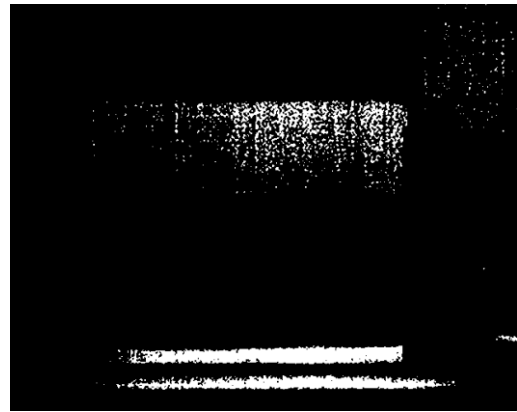
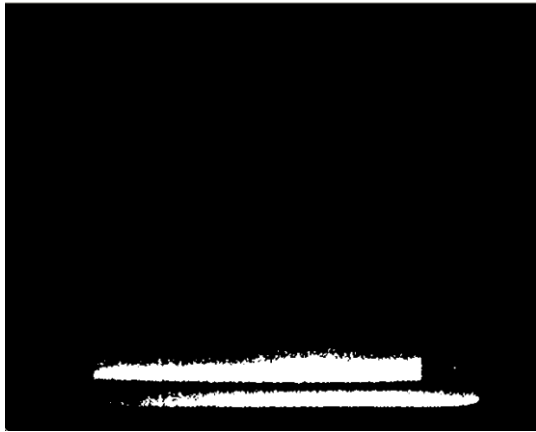


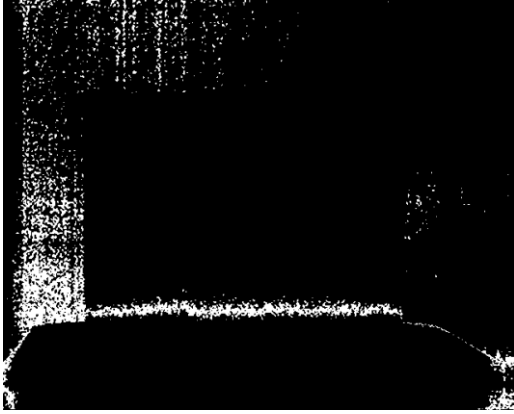


6.2. ANNEX B – Results of using Detect Anomalies









6.3. ANNEX C- Result of using Detect Colors

